ENHANCING ENERGY GENERATION FROM BIOMASS RESOURCES USING THE PYROLYSIS PROCESS ON ANIMAL MANURE

by

Mohamed Maache

A Thesis Submitted in

Partial Fulfillment of the

Requirements for the Degree of

Master of Science

in Engineering

at

The University of Wisconsin-Milwaukee

December 2023

ABSTRACT

ENHANCING ENERGY GENERATION FROM BIOMASS RESOURCES USING THE PYROLYSIS PROCESS ON ANIMAL MANURE

by

Mohamed Maache

The University of Wisconsin Milwaukee, 2023
Under the supervision of Professor Ryoichi S. Amano

In the U.S. and globally, the increase in energy demand and the high cost of fossil fuels have prompted the search for alternative ways to fulfill the energy demand. Biomass is the ultimate energy resource for fossil fuel independence, cost-effectiveness, and climate change mitigation. This paper presents a study of different biomass resources and the processes used to convert organic materials to clean, renewable energy in the most effective way possible. The paper focuses on the thermochemical process of pyrolysis that uses Thermogravimetric Analysis (TGA) and the Differential Thermal Gravimetry device (DTG) from Shimadzu DTG-60AH. This process conducted in this study is based on the pyrolysis of horse manure, which is undertaken with eight different heating rates. It is found that the most efficient and feasible heating rates are the slower ones below 15°C per minute. Also, this study investigated a comparison between horse manure and other types of animal manure: chicken, cow, and sheep. Horse and sheep manure share similarities in thermal degradation temperatures. Chicken and cow manure also have similar temperatures for the threshold of thermal degradation and differ significantly from the thermal degradation threshold of horse and sheep manure.

Dedicated to:

My father Ahmed, my mother Nora Halak, my sisters Romaissa, Djihad, and Rofaida. My brothers-in-law Tahar and Hocine. My nieces Renad and Israa, my nephews Mohamed and Ahmed. To Alan, Allegra, Jean Yahiaoui and Sonia. To all my friends in the U.S. and overseas.

Page intentionally left empty

TABLE OF CONTENTS

LIST OF FIGURES

LIST OF TABLES

ABBREVIATIONS

A	Pre-exponential constant in Arrhenius equation
ADF	Acid detergent fiber
CP	Crude protein
Btu	British thermal unit
DTA	Differential Thermal Analysis
DTG	Derivative Thermo-Gravimetric
DM	Dry matter
DE	Digestible energy
E	Energy
E_a	Energy of activation
GHG	Greenhouse gases
J	Joules
K	The rate constant of the reaction
k	Reaction rate
NDF	Neutral detergent fiber
NSC	Non-structural carbohydrates
m	mass
n	Order of reaction
t	Time

TGA	Thermo-gravimetric analysis
W	Mass of biomass

GREEK SYMBOLS

α	Extent of reaction
β	Linear heating rate
Δ	Change
ρ	Density

SUBSCRIPTS AND SUPERSCRIPTS

*	Superscript of normalized values
a	Activation
f	Final
i	Species i
j	Reaction j
o	Iniatial
t	At time t

ACKNOWLEDGEMENTS

Getting this far was the enormous support and faith from my advisor, Professor **Ryoichi Amano,** who's support will never be forgotten. Also, I have received great support from **Osama Selim** whose steps I followed. **Allegra** has cleaned up all my work and improved my language skills. Alan assisted me in some basics of biology. Professor Hiroyuki **Kumano**, greatly participated in this study with generating the programing part and the theoretical results. Professor Brooke **Slavens** provided help with revising the thesis and clarifying several points. I am grateful to Professor William **Musinski** for taking his valuable time to be part of the committee.

I was never walking alone during every single step of this journey. I would like to show my gratitude to those who have been walking with me and pushing me forward during this journey.
From my lovely **family** that I love with all my heart: My father Ahmed Maache, My mother Nora Halak, My sisters Romaissa, Djihad, and Rofaida. My brothers-in-law: Tahar Bachi and Hocine Benayache.
Also, my **American parents, Allegra and Alan**. **Yahiaoui** family **Mohamed** and **Hassiba**. The **Creighton** family Jolien, Philip, Alexander and especially **Jean**. Wilkistar Otieno.

From my **friends** who also have had my back always and pushed me hard forward: Ahmad **ELHadi**, Abdel Rahman **Salem**, Omar **Habash**, Yusuf **Yahia**, Oussama **Aouali**, Saif **Al Hamad**, Ahmed **Shaker**, Shahad **Hafez**, the twins Cheikh and Kada **Kada**, José Angel **Bugarin**, Faizan **Mahmood**, Mohamed **Qandil**, Francesca **Bollani**, , Yusur **Yahya**, Anis **Adjroud**, Becca **Yang**, Joaquin **Perez**, Josseling and Marling **Martinez**, Jenny **Martinez**, Michael **Madlock**, Betsabell **Gourcuff,** Mona **Saiid,** Cynthia **Reyes,** Sabrina **Benali.**

To all my instructors and professors during the graduate and undergraduate level. For my home country, Algeria, because of unconditional love.

Finally, I would like to acknowledge the funding from the US Department of Energy under DE-EE0009728 for the support of my research.

Chapter 1: Introduction

Today's modern world relies overwhelmingly on energy, powering everything from lights to communication devices. As the population increases and more technology is developed, more energy is needed to meet the demand. From the beginning of human existence, the energy demand has greatly increased, leading to total dependence on fossil fuels such as oil, coal, and natural gas. Renewable energy has only fulfilled a small quantity of the global energy demand in the last few decades.

In 2021, according to the Energy Information Administration, the United States' primary energy consumption was around 98 quadrillion Btu, which comprised 16% of the world's primary energy consumption (equivalent to approximately 604 quadrillion Btu). 79% of the United States' energy consumption was from fossil fuels, 12% was from renewable energy, and 9% was from nuclear reactors [1].

This massive energy reliance on fossil fuels is alarming for many reasons: the finite amount available for these resources, the rapid increase in energy demand, and the high pollution caused by these harmful gases, specifically CO2, which are emitted when burned.

In response to these global issues, there has been a shift toward renewable energy sources such as geothermal, solar, hydro, wind, and biomass. These energy sources still present challenges such as air pollution and land usage; for example, implementing solar panels and wind farms requires a huge land surface. In addition, there are also negative effects on wildlife, such as when the blades of wind turbines kill birds and when the blades of hydro turbines kill fish. However, the damage from energy obtained from renewable resources is drastically lower than from fossil fuel sources. In the United States, wind energy is the largest renewable energy resource, providing 27%; both hydroelectricity and biofuel come in second with 19% each; wood with 17%; solar with 12%; and finally, biomass from waste and geothermal respectively with percentages of 4% and 2% [2].

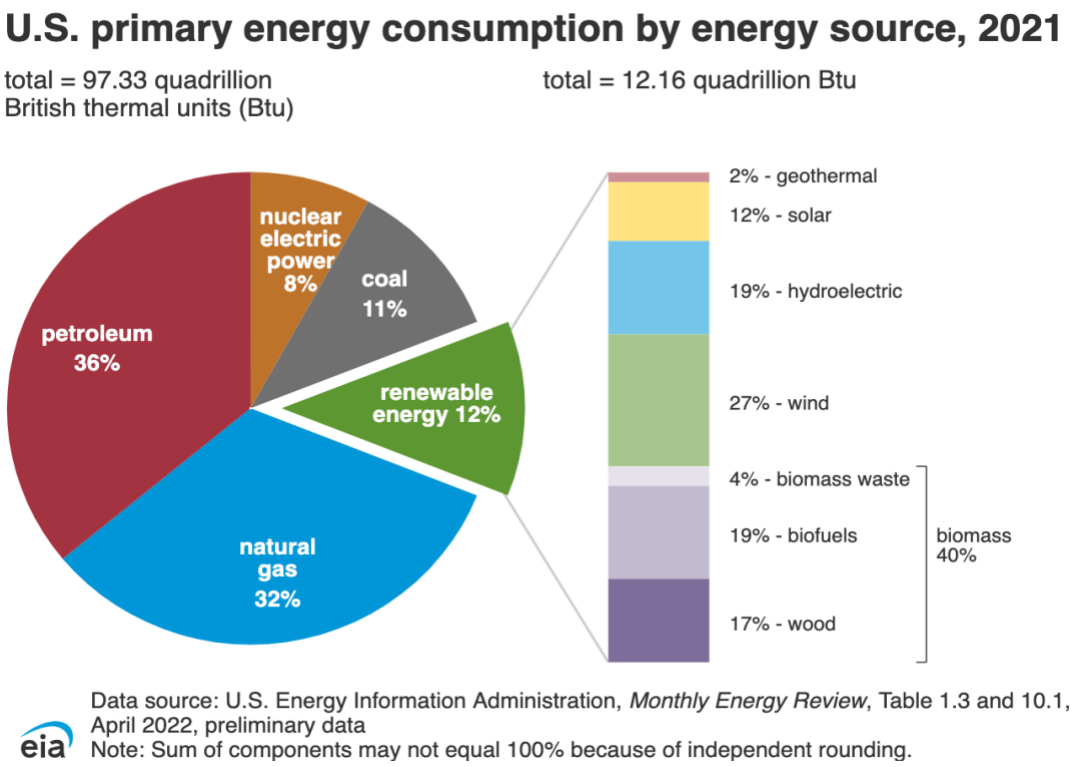

Figure 1: U.S. primary energy consumption by energy source [2]

Biomass is the most widely available resource used since the beginning of humanity. Living organisms, like plants, receive energy from the sun which is stored as chemical energy. This energy can then be converted into biofuels and is referred to as biomass feedstock. Other biomass feedstock sources include municipal solid waste, human sewage from wastewater treatment plants, and animal manure, which can be converted into biogas [3, 4].

1. Reasons to Use Biomass Energy: Sustainable and Renewable

1.1. Waste Management and Reduction

Biomass can potentially reduce the amount of organic waste in landfills by turning it into a valuable renewable energy source. This reduction in organic waste, including disposal and landfill usage, is used as feedstock for biomass energy, which can significantly lower the amount of waste needed for management. This waste reduction not only saves space from landfills but also decreases

the amount of methane emitted by the anaerobic decomposition of the organic waste [5]. Over a span of 20 years, methane will absorb 86 times more heat than carbon dioxide [6].

1.2 Pollution

Currently, fossil fuel energies emit greenhouse gases, which trap heat and contribute to global warming. The main greenhouse gases include carbon dioxide (CO2), methane (CH4), nitrous oxide (N2O), and fluorinated gases. These gases allow sunlight to penetrate the atmosphere via radiation heat transfer but prevent some heat from escaping back into space. As a result, according to the Intergovernmental Panel on Climate Change (IPCC), the earth's average temperature has increased by 1.5°C above pre-industrial's period temperature, which has caused massive disruptions in climate change. The IPCC expects an increase of 0.2°C every decade with the continuous greenhouse gases emission to the atmosphere [7].

Carbon dioxide, or CO2, is the main greenhouse gas released due to human activity and industrial processes such as burning fossil fuels [8]. Methane, or CH4, is emitted from the decomposition of organic waste in landfills, livestock farming, and certain animals' digestive processes. Nitrous oxide, or N2O, is released from agricultural and industrial production and the combustion of fossil fuels and solid waste. Finally, fluorinated gases are hydrofluorocarbons (HFCs), perfluorocarbons or PFCs, and sulfur hexafluoride or SF6. Alternatively, biomass energy can help reduce greenhouse gas emissions by reducing the waste decomposition in landfills by burning fewer fossil fuels [9].

Finally, the fossil-fuel extraction techniques such as offshore drilling and fracking, the transportation across oceans and countries, and the process of converting the extracted fuel to useful energy has an enormous impact on global warming and water contamination.

1.3 Renewable

Considering the wide availability of biomass, these resources are under-utilized. Unlike fossil energy sources, biomass is a renewable energy source that ensures continuous feedstock production as it can be replenished [10]. Reforestation is an example of a renewable resource of feedstock. Even though it could take at least 4 years for bamboo trees to grow, it could be a solution to diversify sources of energy. Also waste acquisition, such as animal manure from farms and dairy operations and human and industrial waste production, provides a continuous renewal of biomass stock. In addition, biomass energy is ubiquitous because it is not limited to certain areas but widely spread throughout the world. In contrast, fossil fuels are located in specific parts of the world where acquisition is based on geopolitical forces. This imbalance in availability creates political conflicts and energy resource monopolies worldwide. It also requires the transportation of polluting fuels across oceans and borders, which cause harm to marine life and wildlife [11-13].

2. Resources

Biomass energy resources are organic materials derived from living organisms that can be used as renewable energy sources. Biomass is a clean, renewable energy promising potential to replace fossil fuels. Only in the United States can 1.3 billion tons of biomass be harvested annually without notable changes in land usage and interference in food grain production. Only the U.S. consumes over 7 billion barrels of oil annually as an energy source. 3.7 billion barrels of fossil fuels can be replaced by harvesting 1.3 billion tons of biomass for the same amount of energy [14]. Some of the most common types of organic organisms come from crops, forest crops, municipal waste, sewage, and animal manure [15].

2.1 Agricultural Crops and Residues

Biomass energy is a clean, renewable energy source that includes food crops from corn, sugarcane, corn stalks, rice, barley, maize, soybean, and wheat straw residues. Globally, this biomass source has a yearly production of 3.7 Pg of dry matter. These sources, commonly used in ethanol fuel production, are a decent substitute for gasoline [16]. By 2030, the United States could produce 155 million tons of agricultural residues. Figure 2 shows a projection of the agricultural residues and manure availability by county in the United States in 2030. Most of the concentration of this type of biomass is based in the upper Midwest, which is known for its agricultural production. [17]

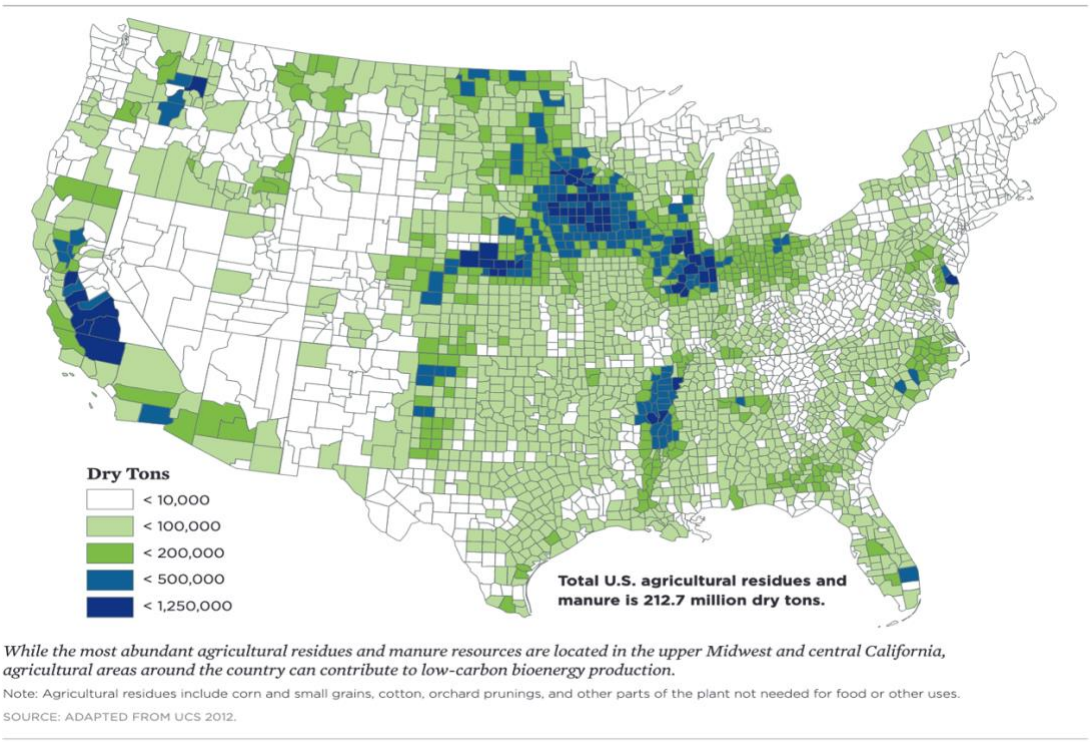

While the most abundant agricultural residues and manure resources are located in the upper Midwest and central California, agricultural areas around the country can contribute to low-carbon bioenergy production.

Note: Agricultural residues include corn and small grains, cotton, orchard prunings, and other parts of the plant not needed for food or other uses.

SOURCE: ADAPTED FROM UCS 2012.

Figure 2: Agricultural Residues and Manure Availability Projection in 2030 [17]

2.2 Forest Crops and Residues

Forest Crops are a source of energy production that can be obtained from trees or plants in the forest. The methods for biomass production from forest crops use Short Rotation Coppicing (SRC), which involves the dense cultivation of high-yield willow species. These plants are harvested within

an average cycle of 3 years. A second method uses Short Rotation Forestry (SRF), which involves planting trees and subsequent harvesting once the trees have grown to a size of roughly 10-20 cm in diameter at chest height. This growth process typically takes between 8 and 20 years. Finally, the third method comes from creating wood pellets, small pieces of compressed wood, as biofuels. [18]

2.3 Municipal Waste

Municipal Solid Waste (MSW), disposed items such as garbage or trash, consists of various materials generated by households, businesses, and institutions. According to the EPA, MSW does not include waste from construction and demolition (C&D) debris, municipal wastewater treatment sludges, or non-hazardous industrial waste. According to the EPA, the total MSW-generated material in 2018 in the US was 292.4 million tons.[19] Figure 3 is a pie chart representing the total MSW generated by material type, while Figure 4 breaks down the management of these types of waste.

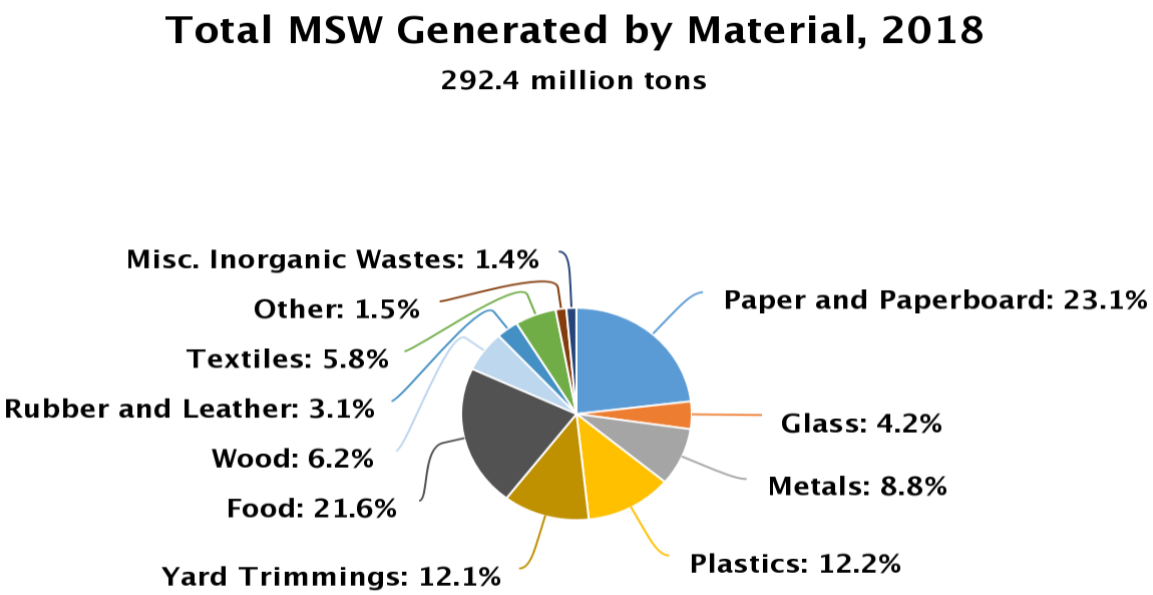

Figure 3: Total Municipal Solid Waste Generated by Material in the US, 2018 [19]

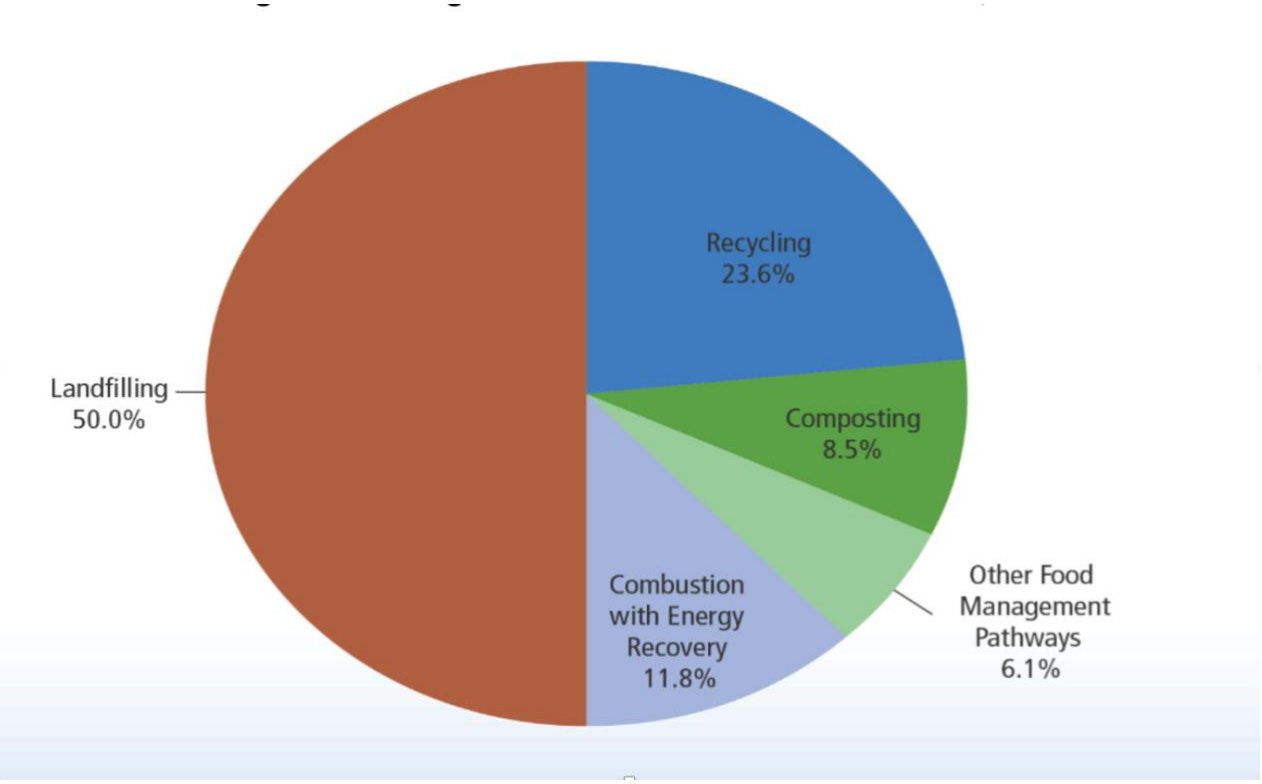

Figure 4: Management of Municipal Solid Waste in the US

2.4 Sewage

Sewage is discharged wastewater from households and industrial and institutional facilities. In the United States, 34 billion gallons of wastewater is processed on a daily basis by more than 16,000 wastewater treatment facilities [20]. One method of converting sewage into energy is through a process known as anaerobic digestion, where biogas is produced by the process of bacteria, which breaks down the organic material in the absence of oxygen [21]. Another method is sludge incineration, where sewage is dried and used as fuel. [22].

2.5 Animal Manure

Animal waste is a byproduct of livestock farming. This organic material has several uses such as fertilizing cropland and gardens using fresh manure directly, which is considered one of the most common uses worldwide [23]. This process must be moderated in order to preserve the soil from contamination. Composting is a process of decomposing and converting animal waste into nutrient-

rich organic matter that can be used in plants fertilization. Animal manure composting has many advantages such as pollution and odor reduction. Animal manure consists of different stages of life of internal parasites that can cause dangerous health conditions. These severe health conditions are prevented by using high temperatures that rapidly destroy the parasitic eggs after reaching the temperature of 104°F [24]. Animal manure is also used as a source of energy. The distinctive characteristic of animal manure is that the wide availability of this energy resource permits it to not only be a powerplant product, but it can also be implemented as a source of energy on a residential scale. According to the United States Department of Agriculture's 2017 Census, the U.S. had about 94.8 million cattle and calves, 74.6 million hogs and pigs and over 3,876 million chickens [25]. The US. has an estimated annual production of dry chicken manure of 12 billion pounds. [26]. The amount of waste produced can be estimated using the single animal generation amount multiplied by the total animal population. A mature dairy cow can produce around 14 gallons (120 pounds) of feces and urine where at least 12% is solid waste [27]. A 1,250-pound beef cow generates 45 pounds of manure daily, while pigs generate an average of 11 pounds [28]. A horse can produce an annual average amount of manure that varies between 9-29 m^3 which is equivalent to 8-14 tons/year of collectible manure. The population of horses in the United States in 2005 surpassed 9 million with 5 million horses in Europe. Horses have a global annual production of between 500-800$\times 10^6$ in which 40-70 $\times 10^6$ [29-31]. The estimate of the total amount of the animal waste produced worldwide is about 3 trillion kg (6.6 trillion pounds) of dry manure. Most of this amount is used directly in agriculture, while some of it is used in producing energy. With an average energy density of 20 MJ/kg, the potential energy extracted from this amount is $3 \times 10^{12} \times 2 \times 10^7 = 6 \times 10^{19}$J ($5.69 \times 10^{16}$Btu) [32].

Chapter 2: Literature Review

Traditional energy resources, such as coal, oil, and natural gas, are the major energy contributors to meet the global energy demand. However, these contributions play a significant role in the increase in climate change around the globe and threaten the existence of humanity. [33] According to the Energy Information Administration (EIA), global energy consumption is projected to increase by 50% between 2018 and 2050 [34].

Biomass encompasses a variety of organic materials used for energy. Its role in modern renewable energy is increasingly important in replacing fossil fuel energies. Therefore, a significant number of studies have been done on the different processes of converting biomass into clean, renewable energy.

Processes

Biomass can be converted into energy through several processes, each of which has its benefits and drawbacks. These methods often depend on the type of biomass feedstock, the desired form of energy output, and various economic and environmental factors. The most appropriate methods for the generation of biomass energy are stated below.

1. **Biochemical Conversion**

This process uses biological organisms such as bacteria and enzymes to break down biomass to produce clean energy [35].

Anaerobic Digestion

Microorganisms break down biomass in an oxygen-free environment to produce biogas (mainly composed of methane and carbon dioxide) and a nutrient-rich digestate [36]. Previous literature indicates that anaerobic digestion effectively converts raw solids and organic waste into the energy in biogas or in other forms. Also, one of the advantages of the process is the low capital cost

[37]. In Stuart's 2006 [38], several process advantages are listed, such as the wide availability of resources, the economic benefit, and the flexibility in scaling up the technology. On the other hand, many disadvantages, such as environmental concerns and fluctuation in load, are also discussed.

Fermentation

Sugar in biomass is converted into alcohol, like ethanol, using yeast or bacteria. Corn and sugarcane are the most commonly used biomass feedstocks [39].

Transesterification

Biomass is used to create biodiesel. Biomass feedstock like vegetable oils, animal fats, or waste cooking oils undergo a chemical reaction, called transesterification, with alcohol to produce biodiesel and glycerol [40].

2. Thermochemical conversion

The conversion of biomass into useful energy uses high temperatures and chemical reactions in the presence or absence of oxygen. Methods in this process are direct combustion, pyrolysis, and gasification [41].

Direct combustion

Direct combustion is the process of burning biomass to produce heat to generate electricity. Direct combustion could produce energy for heating purposes, or it could be used to generate electricity, creating steam that rotates a turbine to convert the kinetic energy into electrical energy by using a generator. Lio et al., 2021, investigated the efficiency of utilizing the combustion process on horse manure as an energy source. The challenge in this process is the heterogeneous nature of horse manure, the wet mixture of bedding materials, and feces, which requires a particular furnace design to function. Also, another issue is the significant presence of nitrogen in the fuel, which often leads to ammonia emission, which is hazardous. A similar study was done in 2009 by Lundgren and

Petterson who found that the emission of carbon monoxide (CO) was between 30-150mg/Nm^3 and the NO_x was between 280-350mg/Nm^3. Suggested solutions in the study were adding other types of biomass, such as wood shavings and sawdust, to improve the process. Also, lower emission of CO is achieved if the water content is kept below 50wt% even though the process of combustion using horse manure is still feasible; however, drying the sample is still a crucial issue [29, 30].

Gasification

Even though combustion is the simplest and most straightforward method of converting biomass into energy thermochemically, it has a lower efficiency in heat generation. Besides, gasification is more efficient and has many more advantages over combustion. Gasification requires less feedstock and converts feedstock into multiple types of energy that could be used for heating, transportation, or power. Gasification has a significantly lower emission of greenhouse gases such as nitrogen and sulfur [42]. In gasification, biomass is partially oxidized by supplying oxygen, air, or steam to the reaction as a gas agent. Biomass is heated, and the reaction produces syngas, such as hydrocarbons [43]. This syngas can be used as a fuel for power generation or further processed to produce biofuels or chemicals. Gasification can convert the burden of the animal manure into fuel participating in fostering energy security and achieving energy sustainability [44, 45]. Amano et al. 2013 [46] conducted a study to utilize carbon dioxide as a gas agent in gasification to decrease the amount of GHG emitted. An experimental investigation was conducted on chicken manure using carbon dioxide as a gas agent to study the effect of the particle size on the residual mass and conversion rate. The results show that larger particles are correlated to lower conversion rates and higher residuals [46]. Amano et al. investigated the evolutionary behavior of syngas composition using pyrolysis with nitrogen being the agent gas and gasification at different temperatures and different oxygen concentration. The different temperatures used were 600°C to 1000°C with an

increment of 100°C. The oxygen concentrations in nitrogen used were 21% and 10% The gas evolved was quantified using a gas chromatography. Amano et al. concluded that higher oxygen concentration (21%) generated higher energy yields versus lower concentration (10%) [47].

In addition, Kumar et al., 2009,[36] states that one of the advantages of biomass gasification is that it occurs at lower temperature than coal gasification because biomass is more reactive. Therefore, greenhouse gas emission is decreased because lower temperatures diminish the extent of heat loss as well as reduce material defects associated with higher temperatures [36]. Trninic et al. [48], in their paper "Biomass Gasification Technology: The State of the Art Overview," conducted an overview of biomass gasification technologies and evaluated their advantages and disadvantages. It was stated that the temperature was the most important parameter to control the operation of the gasification process. Higher temperatures lead to higher gas yield due to the higher conversion efficiency. Besides temperature, other aspects had an impact on the efficiency of the gasification process: the agent gas (oxygen, steam, or air), the equivalence ratio (excess air ratio), pressure, residence time, and the shape and the size of the sample. It was concluded that even though gasification was among the most restrictive processes for converting biomass to energy, it still had many challenges, such as the preheating requirements before the process and the high cost of cleaning the device to prevent contamination [48].

Pyrolysis

Pyrolysis is a thermochemical process of heating biomass in the absence of oxygen, which leads to the decomposition of biomass into solid, liquid, and gaseous products. This process breaks down the complex organic compounds into simpler molecules which is also referred to as thermal cracking. Pyrolysis can produce biochar, bio-oil (also known as pyrolysis oil), and syngas (a mixture of carbon monoxide and hydrogen), which can be further processed into fuels or chemicals [49].

Selim et al. investigated the process at the same lab in 2021 using chicken and cow manure with different heating rates. This study used pyrolysis for each manure type with eight different heating rates of 5-40C°/min. The results showed different temperatures of the thermal degradation for each manure type. For chicken manure, the thermal cracking, which is a chemical process of breaking down large compound hydrocarbon molecules into smaller ones by applying an adequate amount of heat, associated with hemicellulose decomposition occurs at 250°C, while for the cow manure, it occurs at 300°C. For the cellulose decomposition, the thermal cracking temperature occurs at 300°C and 470°C for chicken and manure, respectively. The results concluded that pyrolysis with slower heat rates allows for a quasi-equilibrium state [50]. In another report, Selim et al. investigated the effect of different heating rates and the gas agent type in the thermochemical conversion process. The manure type used in this study was chicken, and the gas agents were nitrogen, air, and carbon dioxide. After conducting a thermogravimetric and differential analysis, results showed that the lowest rates were recommended as they provided adequate time for a quasi-equilibrium reaction. In terms of gas agents, air gasification tended to be the most self-sustainable process as it had a larger temperature range for the exothermic reaction. Pyrolysis using nitrogen also showed a significant range of temperature for exothermic reaction. Moreover, gasification using carbon dioxide showed a more complicated thermal degradation profile [51].

The technique utilized in this study to analyze the data is the Thermogravimetric Analysis (TGA), which measures the weight changes of a sample at a given time and temperature. The device used for this technique is the Differential Thermal Gravimetry (DTG) from Shimadzu DTG-60AH. The difference between the thermochemical processes is summarized in Figure *5*. The main difference is the agent gases involved in the reaction, the heat range, and the final product.

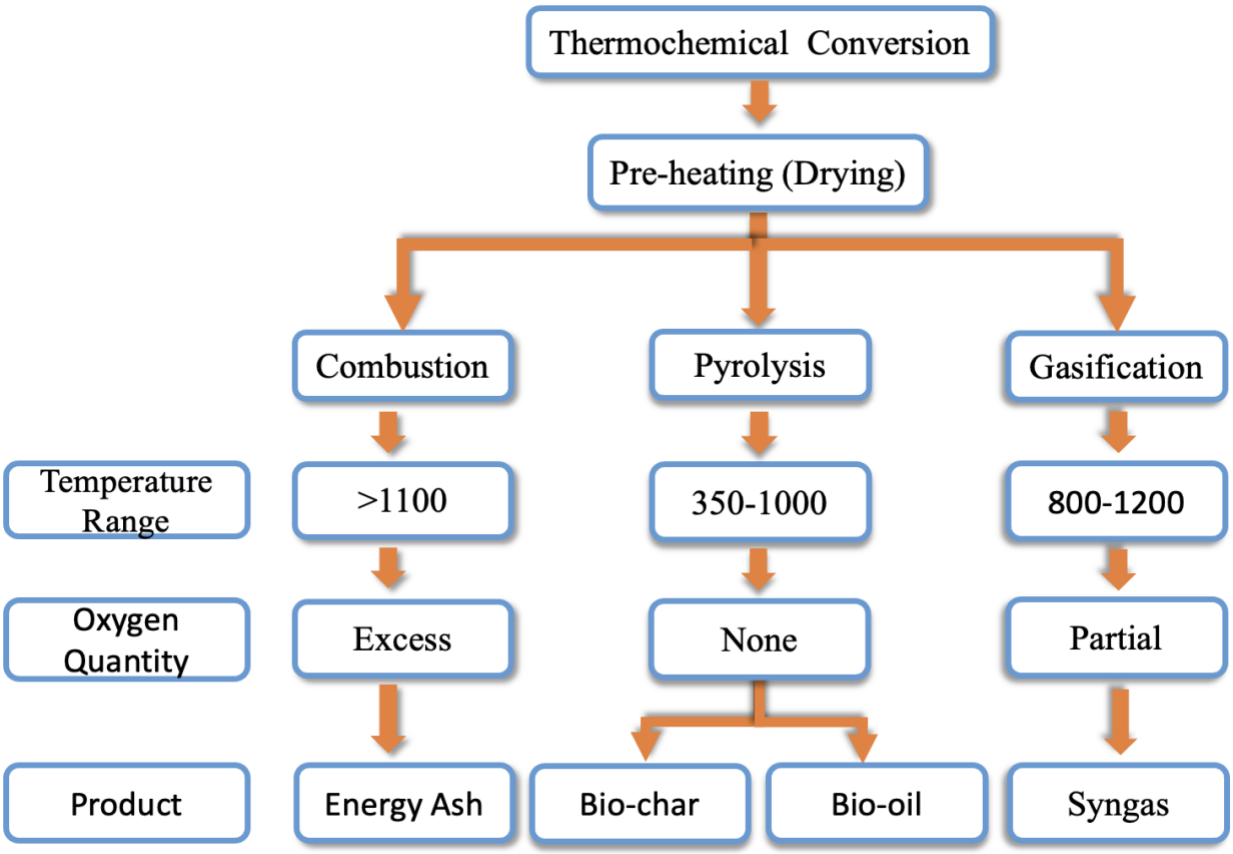

Figure 5: Diagram of the Thermochemical Conversion Processes

The horse manure composition percentages (cellulose, hemicellulose, lignin, and protein) depend on many factors, such as the horse's age, size, activity, and nutrition. 40% of the horse feedstuff consumption is excreted into manure, and feed with higher fiber content, like hay and grass, have a lower digestibility [52, 53]. This study used a sample from the same horse manure to get microscopic images using a 3D-measuring laser microscope OLS4100 from Olympus. Figure 6, which is a microscopic image of the sample, and which shows that the sample consists mostly of fibers and undigested hay with a small amount of partially digested feed and some impurities, as shown below.

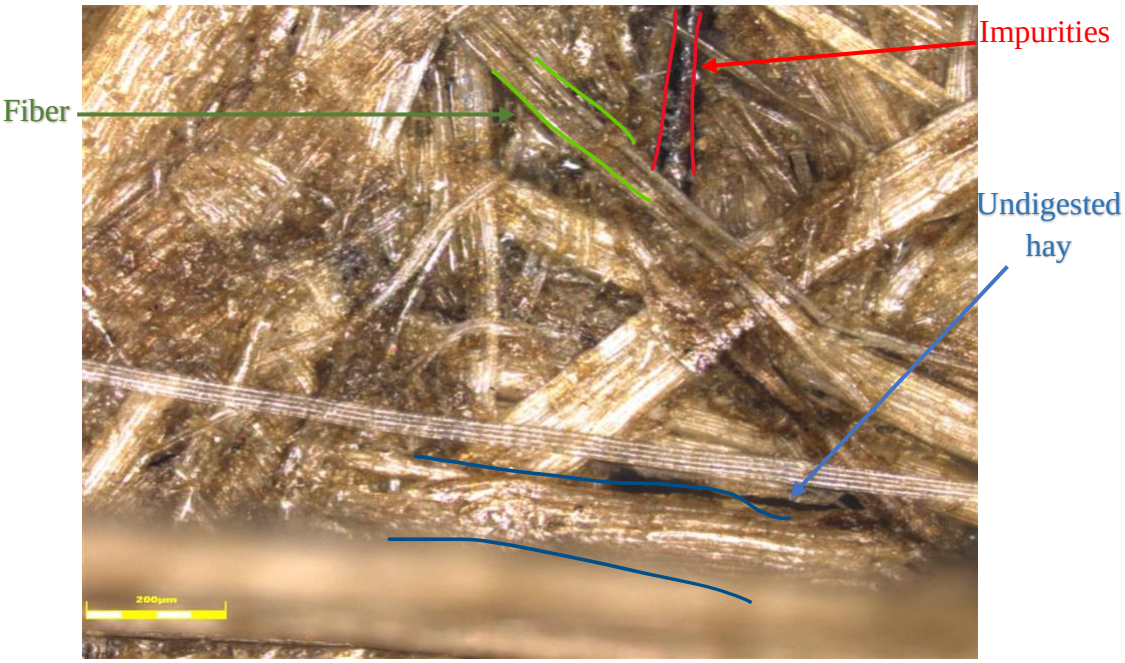

Figure 6: Microscopic Image for Horse Manure at 200µm Scale

Knowing that horse manure consists mostly of hay, the chemical composition of horse manure can be explained using the chemical composition of hay. A study has been done on a sample from horse feedstock by Danielle Smarsh in an article titled, "Understanding a Hay Analysis." This article reveals the specific quantities of the different nutrients available in the hay. The analysis is done in a particular laboratory, and the results are summarized in Table 1 [54].

Table 1: Chemical Compositions for Dry Hay with Their Percentage of Availability [54]

Term	Meaning	Typical Value
DM	Dry matter: The nutrients without water	85%
Moisture	The amount of water in the hay	11-16%
CP	Crude protein: The amount of protein in the hay	8-20%
ADF	Acid detergent fiber (cellulose + lignin): a measurement of the fiber	30-45%
NDF	Neutral detergent fiber (hemicellulose + Cellulose + lignin): a measurement fiber	40-65%
NSC	Non-structural carbohydrates: a measurement of simple sugar and starch the subset of this includes WSC, ESC, and NFC	5-25%
DE	Digestible energy: The amount of energy digested and used by the horse	0.75-1.0 Mcal/lb

The sample of hay taken for the analysis is dried completely of its urine and other liquids before the analysis. The water content percentage represents the water in the inner structure of the cells. As seen in the table, the main component of the hay is **moisture,** which makes up about 11 to 16% of the total mass. A lower percentage of water content, lower than 10%, would lead to the loss of nutrients. **Crude protein**, which ranges between 8% and 20% of the total weight, is mostly consumed by the horse, where the consumption depends on the animal's age and degree of activity. **Carbohydrates,** specifically structural and non-structural carbohydrates, make up the remaining percentages. Both types are technically fibers made of lignocellulosic compositions (hemicellulose, cellulose, lignin) [45]. The analysis done in this research study focuses on the percentage of carbohydrates in the hay as it was the energy source in the experiment's samples. The microscopic image of the samples from the horse manure showed a majority of fiber.

Chapter 3: Mathematical Relation and Procedure

Experimental Setup

The Differential Thermal Gravimetry (DTG) DTG-60AH is the main apparatus for running experiments for this research study. The apparatus consists of the DTG and requires using at least one gas tank, a gas flow control unit, and a computer equipped with data acquisition system software. Figure 10 shows the configuration of the apparatus from Shimadzu used in this research experiment at the Global Water Center, a lab in the University of Wisconsin-Milwaukee [55].

The DTG-60AH

The DTG-60AH is a Shimazu product consisting of a sample holder, balance, furnace, and temperature controller.

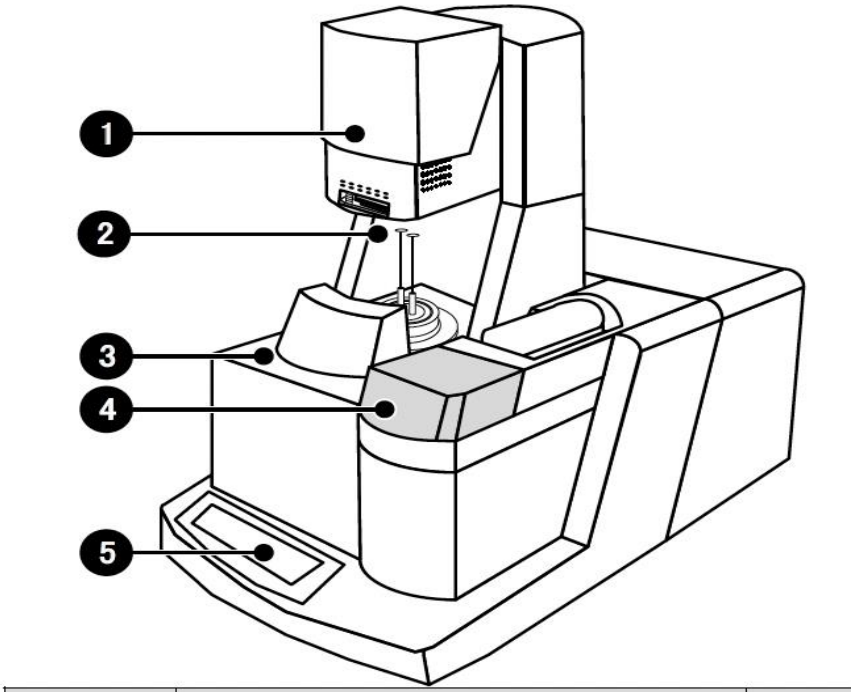

Figure 7: DTG 60 AH Components [55]

Table 2: DTG 60AH Parts and Components [55]

No.	Name
1	Furnace cover
2	Detector and reference rods
3	Tray for setting sample pans
4	autosampler
5	Kay/display section

Sample Holder

The sample holder is a relatively small crucible made of different materials depending on the process, the sample used, and the desired temperature. In this research topic, the alumina pan is used because it can resist the desired temperature of 1,000°C without causing any damage to the pan. Two pans are needed in the device to proceed with the experiment; one is for the sample, and the second is left empty for reference. Figure 8 below shows the sample holder types, including the alumina used for this research experiment.

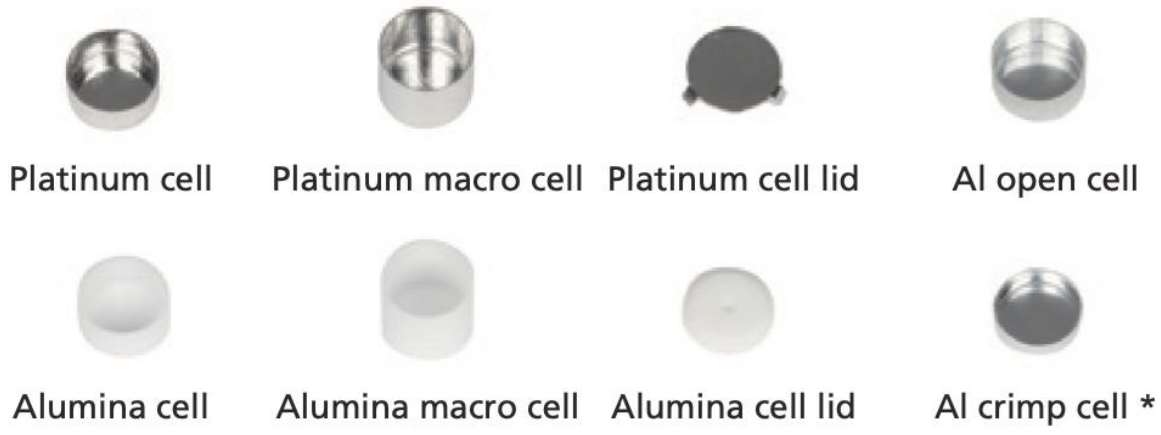

Figure 8: DTG Cells (Pans) Types

Balance

The DTG device is known for high-precision balance. The pans are placed on two rods; the one on the right side is a balance on which the sample is placed, and the other rod is used to counterbalance the weight and provide reference as shown in Figure 9. The degradation in the mass of the sample is recorded continuously. Besides weight, heat is also measured by the sensors implemented in each rod. The sensors are extremely sensitive. Thus, during the sample placement or discharge, the user must do so cautiously to avoid applying force on the rods. The estimated time for replacement and calibration can take more than 60 days.

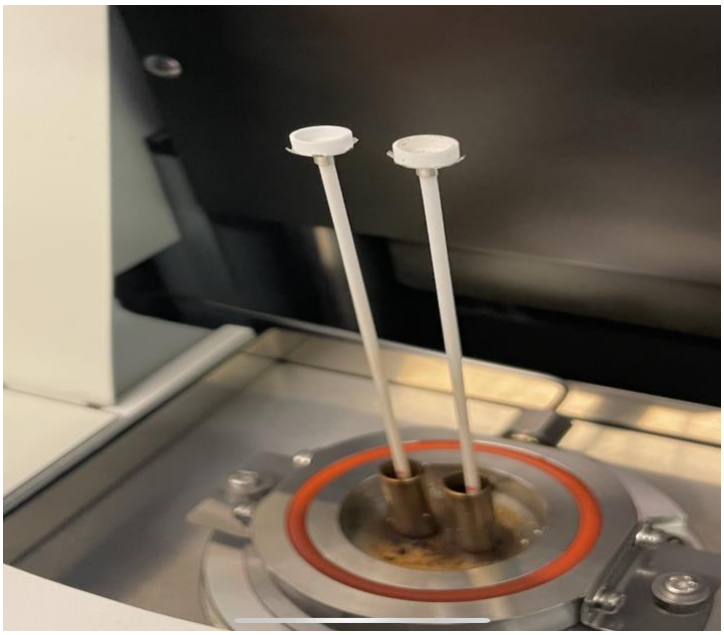

Figure 9: Thermocouples Sensors and Balance Rods

Furnace

An electric furnace is a chamber used to heat the sample and reference the desired temperature at a specific rate of heat. The chamber has one degree of freedom on the y-axis in order to open and close. The opening and closing of the furnace can be controlled manually by the device as long as the temperature is below 100°C, but it is not recommended to open the furnace if the temperature is higher than 50°C.

Gas Flow Control Unit FC-60A

It is a device that connects the gas tanks to the DTG and controls the gas input as needed. The gas flow rate can be controlled manually using the gas flow controller knobs; for this study, the recommended flowrate used for a better performance of the DTG is 50 ml/min. The device has two intakes in order for the device to operate. The necessary intake for the operation is nitrogen or possibly argon, while the second intake, an optional one, is for other agent gases. For this study, nitrogen gas was used with the pressure in the range of 45 psi. The pressure is not controlled from the flow rate but is controlled at the level of the gas tanks using pressure regulators. The device is shown in Figure 10 as a Flow Control Unit model FC-60A.

Software

The software used for this research is LabSolutions TA. For the experiment, the software controls conditions such as temperature, the heat rate increment, the type of pan used, the gas flow rate, and the type of gases. The software generates both DTA and TGA graphs simultaneously. Figure 10 also shows other components of the set-up which is a computer equipped with software LabSolutions TA.

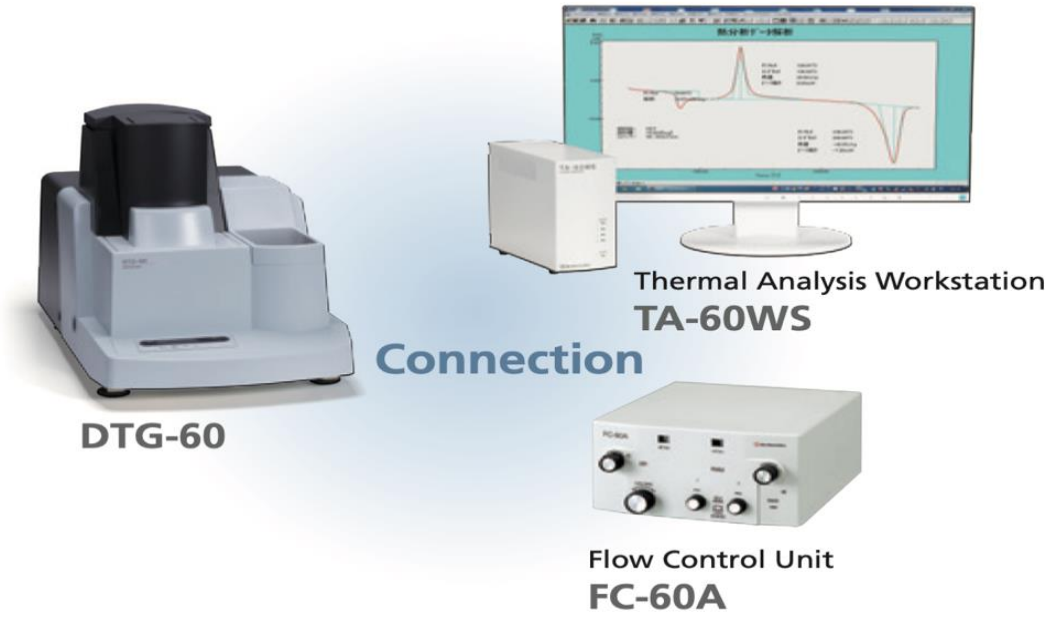

Figure 10: Apparatus Configuration [55]

Figure 11: DTG-60AH From Shimadzu in The Global Water Center UWM

Two techniques run simultaneously within the device that runs this experiment. These two techniques are the **Thermogravimetric Analysis (TGA)** and **Differential Thermal Analysis (DTA)**. In the TGA, the mass of a sample is measured as it changes with temperature or time in a controlled atmosphere. This technique is used to determine a material's thermal stability and the composition of its components. The TGA can identify the temperature where a sample undergoes weight loss. The TGA curve displays the sample's loss or gain of mass as a function of temperature and time. However, in the DTA, the difference in temperature between a sample and an inert reference material is measured when both are subjected to identical temperature cycles in a controlled atmosphere. The sample's temperature will rise or fall at a different rate than the reference material's in response to an endothermic or exothermic event. These differences in temperature between the sample and the reference are recorded as a function of temperature or time, which produces a DTA curve that can provide valuable information about the sample's phase transitions and other thermal properties. The device uses small material samples for many applications, such as the analysis of polymers, the determination of thermal stability, the study of decomposition kinetics, and the characterization of materials such as biomass for energy applications. In the biomass field, the DTG can be used to understand biomass thermal degradation behavior; this is valuable for enhancing the process of converting biomaterial into useful renewable energy through a thermochemical conversion process such as combustion, pyrolysis, or gasification. The DTG-60AH decomposes the organic material at high temperatures. The device functions between room temperature and up to 1,100°C with different heat rates [56].

Mathematic Equations

The device generates a degradation of mass quantity versus time. The extent of the reaction is found using equation 1, which is the ratio of the difference between initial and instantaneous mass and the difference between initial and final mass.

$$\alpha = \frac{w_0 - W_t}{w_0 - w_f} \text{ (Equation 1)}$$

Equation 2 is used to calculate the rate of change of the extent of the reaction, which is the difference between the extent of reaction at instant and the previous data point.

$$\frac{d\alpha}{dt} = \frac{(\alpha_t - \alpha_{t-1})}{\Delta t} \text{ (Equation 2)}$$

Equation 3 is the Arrhenius equation, which is named after the Swedish chemist Svante Arrhenius. This relates the rate of the chemical reaction to the temperature and the activation of energy of the reaction, which is the amount of energy needed to start the reaction.

$$k(T) = A \exp\left(\frac{-E_a}{RT}\right) \text{ (Equation 3)}$$

Equation 3 is for the constant of decomposition rate k where A is the pre-exponential factor, R is the gas constant, and T is the absolute temperature.

Using equations 2 and 3, equation 4 is generated where β is the heating rate. For this experiment the heating rates used are 5, 10, 15, 20, 25, 30,35, 40°C/min [51]. In equation 5, n value is obtained based on the graph generated from the extent of the reaction to 3 for the polynomial derivative estimation.

$$\frac{d\alpha}{dT} = \frac{k(T)}{\beta} f(\alpha) = \frac{A}{\beta} \exp\left(\frac{-E_a}{RT}\right) f(\alpha) \text{ (Equation 4)}$$

$$\frac{d\alpha}{dT} = k(T)(1-\alpha)^n \text{ (Equation 5)}$$

$$\frac{d\alpha}{dT} = \frac{k(T)}{\beta} f(\alpha) = \frac{A}{\beta} \exp\left(\frac{-E_a}{RT}\right) (1-\alpha)^n \text{ (Equation 6)}$$

$$ln\left(\frac{\frac{d\alpha}{dT}}{(1-\alpha)^n}\right) = \ln\left(\frac{A}{\beta}\right) - \left(\frac{E_a}{RT}\right) \text{ (Equation 7)}$$

Chapter 4: Results

1. Experimental results

The experiment was conducted using the DTG to run Thermogravimetric and Differential Thermal Analysis on horse manure with eight distinct heating rates starting from an ambient temperature of up to 1,000°C. The sample for each run came from a small amount of horse manure ranging between 10 to 30 mg collected from the same animal from a farm in Wisconsin. For the pyrolysis technique, the agent gas utilized in the experiment is nitrogen with the absence of oxygen**.** Figure 12 shows the horse pyrolysis extent of reaction curves for the eight different heating rates: 5, 10, 15, 20, 25, 30, 35, and 40°C per minute. The device starts collecting data at 150°C instead of at room temperature. From room temperature to 150°C, the previous interval is for drying the sample and for moisture evaporation since the sample is utilized immediately after it is taken out of the freezer containing frozen water. In order to achieve better results, the sample has to be preheated to dry it; the process is called torrefaction where the biomass is heated to around 300°C for a dry sample [57]. Data collection on a dry sample provides more accurate results and prevents fluctuation, specifically in the mass' change. The collected data is only taken after the moisture evaporation phase, meaning at the temperature of 150 °C. At this temperature, the initial mass is at the maximum and the extent of the reaction is 0 . At the temperature of 1,000°C, the final mass is at its minimum and the extend of the reaction is equal to 1, meaning no further reaction could be achieved.

From the graph, it is observed that all the curves follow the same trend with different latencies. There are four main stages of the pyrolysis reaction that can be identified. The first stage is for the thermal cracking, and it takes place starting at 200°C. The second stage is for the faster reaction with a higher slope in a temperature range between 200°C and 350°C for the hemicellulose and cellulose mass degradation. The third stage, between 350°C and 780°C, is for the thermal degradation of the

hemicellulose, cellulose and lignin. The fourth stage after 780°C is for a steady reaction. It is also observed that at the temperature of 490°C and a heat rate of 5°C/minute, 90% of the reaction is completed, and 90% of the initial mass is decomposed.

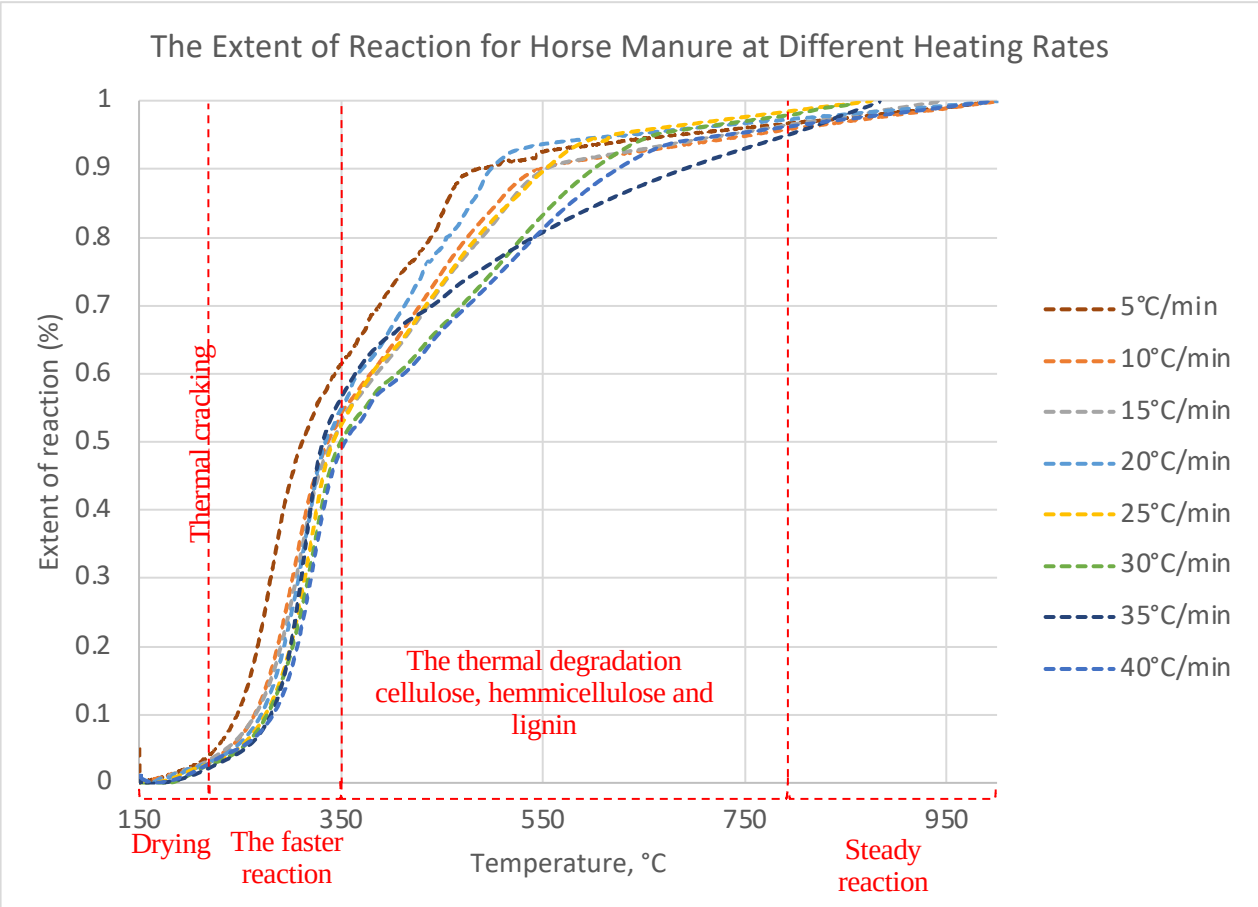

Figure 12: The Extent of Reaction vs. Temperature for Horse Manure at Different Heating Rates

Figure 13 is a graph that shows the rate of change of the extent of the reaction. The eight curves follow a similar trend with a delay in different heating rate peaks. The peaks represent the mass degradation due to the thermal cracking for the chemical compounds that make the compositions of the horse manure. since horse manure is dominantly made of hay the displayed results in the graph are expected. Two main peaks in the graph represent the thermal degradation of the samples' main organic compositions: cellulose and hemicellulose while there is a small amount of lignin in the

sample as shown in the graph with a very small peak at higher temperatures. The first peak for the eight different rates represents hemicellulose and cellulose thermal degradation, which occurs at 270°C and 335°C. For the heating rate of 5°C/minute peak, hemicellulose and cellulose thermal degradation occurs at the temperature of 270°C. The second peak to appear moving to the right is for the 10°C/minute heating rate, where the thermal degradation occurs at the temperature of 286°C. The next peak is for the 15°C/minute heating rate, where thermal degradation occurs at the temperature of 293°C. The remaining curves follow a similar pattern with a shift in the thermal degradation temperature toward the right due to the increase in the heating rate. The trend represented by the 35°C/ minute shows a slightly different behavior in which the peak is at a lower temperature that it was expected, meaning that the thermal degradation occurs at a lower temperature. This means that there was enough time for the heat transfer to allow the reaction to be completed. Even though the 35°C/minute peak is expected to occur at higher temperature, it occurs in this experiment at the same temperature as the 15°C/minute. Also, the peak's magnitude is expected to be lower than the one at 40°C/min. After an investigation into the raw data, it was noticed that the sample associated with the heating rate of 35°C/min had the highest mass. All the other seven samples fell under the same range of mass after drying the manure except for the sample of 35°C/min where it was more than double. The peak still appears at the expected range of temperature and this slight change is due to the faster reaction because of the adequate availability of mass. In conclusion, increasing the heating rate delays the thermal degradation of the sample composition due to the lack of time for a complete reaction.

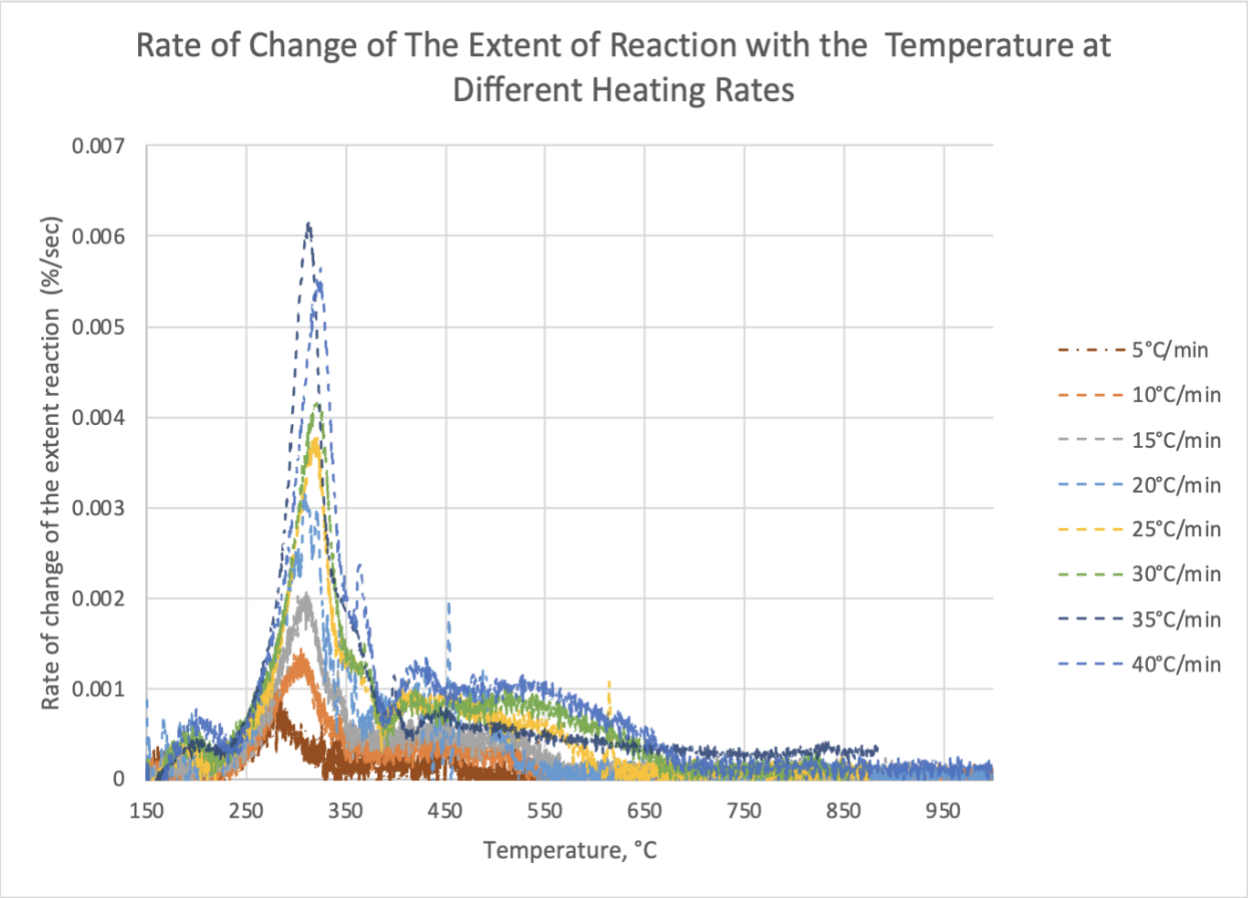

Figure 13: The Rate of The Extent of Reaction vs. Temperature for Horse Manure at Different Heating Rates

Figure 14 shows the DTA variation with the temperature for the eight heating rates. According to the figure, all the heating rates follow a similar pattern in terms of the number of peaks and the temperature range of peaks with small peak variations. Notably, the trends are exothermic in a specific range of temperatures and endothermic in the rest. The 5°C /min curve is the most stable among the eight different curves and is the curve with the widest range of temperature of positive energy from 150°C to 490°C. 10°C/min and 15°C/min are also stable; however, they have a smaller range of endothermic temperature. The sharp decline after the first peak implies higher heating rates where the reaction switches to an endothermic reaction. In conclusion, the reaction is most self-sustainable with a heating rate of 5°C /min at a range of temperature up to 490°C.

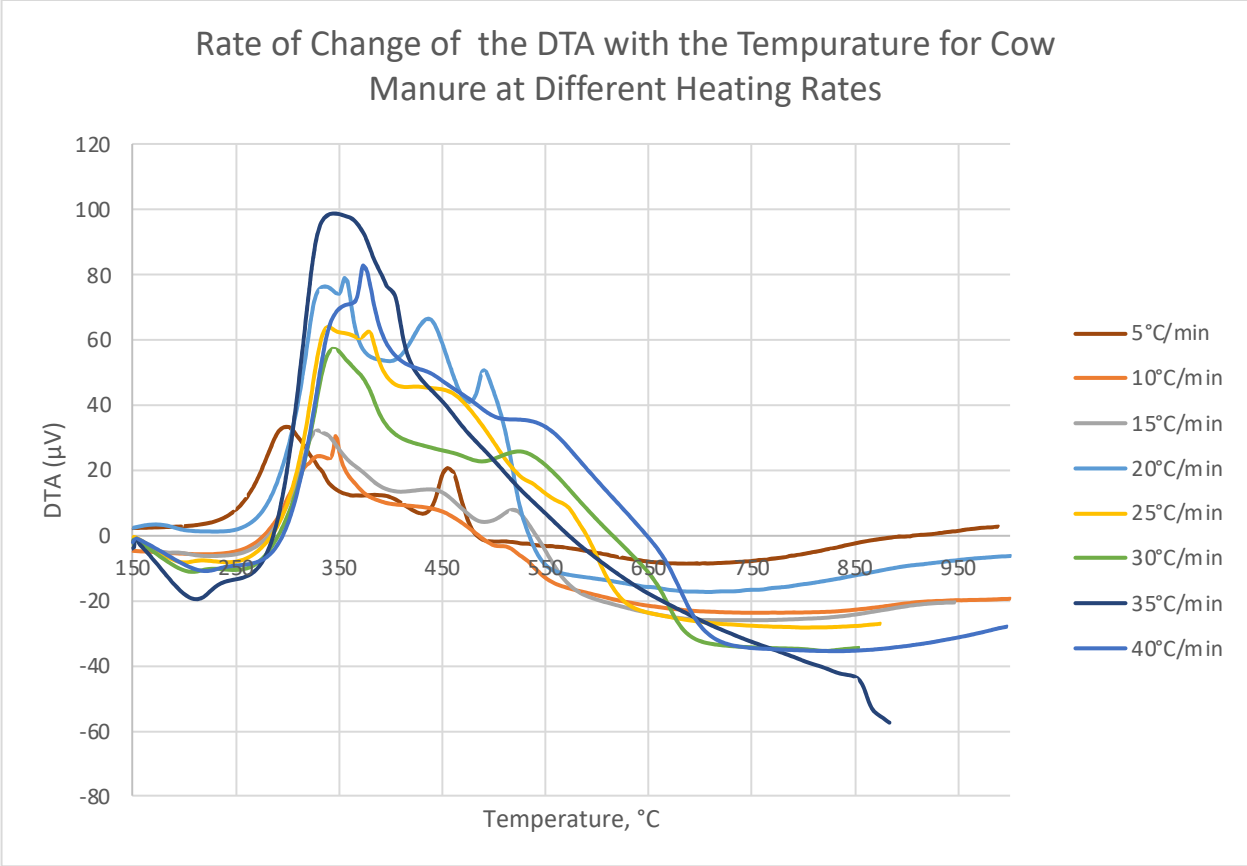

Figure 14: The Rate of DTA vs. Temperature for Horse Manure at Different Heating Rates

One of the objectives of this study was to seek an ultimate mixture of types of manure to develop sustainable energy. Data was taken from the horse pyrolysis experiment and compared to three different types of animal manure. It was observed that the thermal degradation of animal manure occurs at different temperatures. Figure 15 is the graph that represents the rate of the extent of reaction vs. temperature for different types of animal manure, including horse, chicken, cow, and sheep, at a heating rate of 20°C/min. At around 320°C, the first peak occurs for sheep and cow manure, representing the thermal cracking for cellulosic bonds. At the temperature of 270°C, the chicken manure's peak occurs, which represents the hemicellulose thermal degradation of chicken manure where the cellulosic bonds' cracking occurs. Another peak follows directly after for chicken manure at a temperature of around 320°C, which represents the thermal cracking of cellulose.

However, for horse manure, the thermal cracking for the cellulosic bonds occurs at the temperature of around 300°C. For the lignin thermal cracking, it appears late for cow manure at around 800°C, for the sheep manure at around 850°C, a very low peak for chicken lignin at 750°C, and finally horse manure has no peak for lignin because it is the animal manure with the least amount of lignin in its chemical composition.

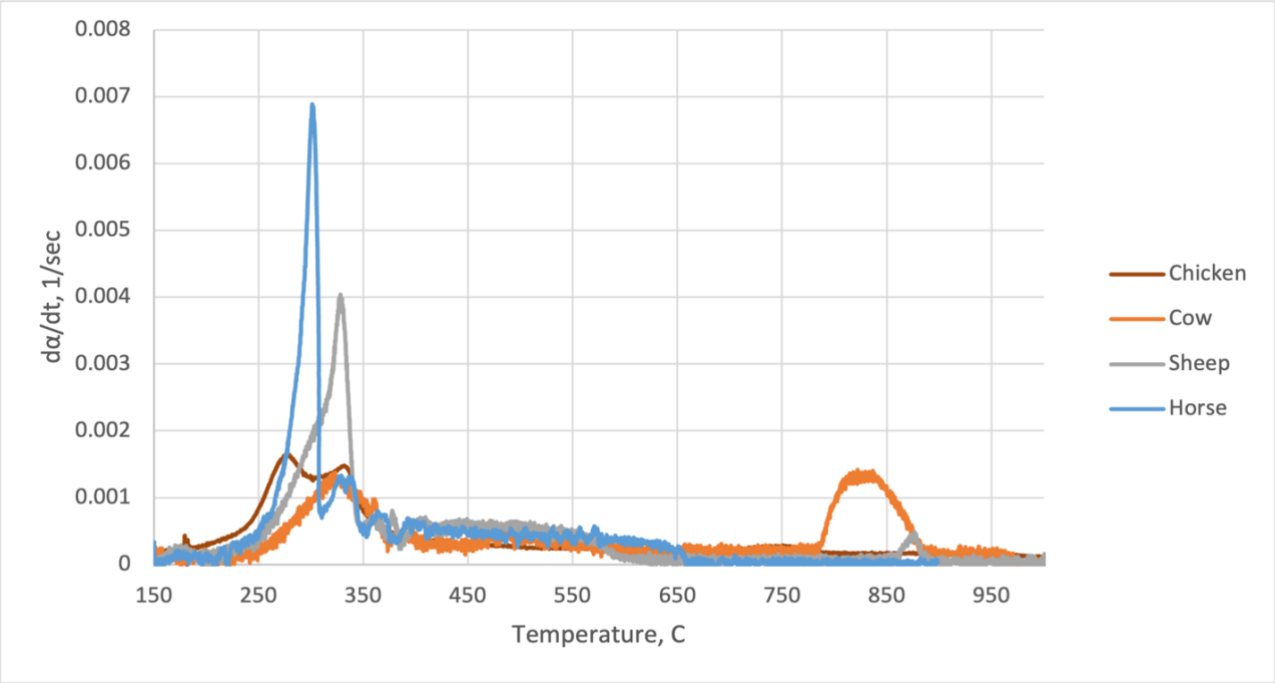

Figure 15: The Rate of Extent of Reaction vs. Temperature for Different Types of Animal Manure

2. Validation of Experimental Results

To evaluate the characteristics of the waste, it is important to predict the mass variation and the heat amount for manure during pyrolysis. In this report, the theoretical calculations for the mass variation during the pyrolysis process were attempted as the first step in conducting the theoretical analysis of the horse manure. At first, the overall kinetic reaction parameters and the Arrhenius equation were used to compare the experimental and the theoretical results. Then, while using the

analytical model proposed by Miller et al., the comparison between the experimental and the hypothetical results and the availability of the analytical model were evaluated [58].

2.1 **The Overall Kinetic Reaction**

In this study, the analytical model proposed by Miller et al. was used [58]. Figure 16 shows the concept of the chemical reaction process in the model. In this model, the composition of cellulose, hemicellulose, and lignin in the biomass are given as the calculation parameters, and the decomposition process for each composition is calculated using the reaction process. K_j is the reaction rate for each reaction process, and the reaction rate can be found by using the equation (8).

$$K_j = A_j \exp\left[\frac{-E_j}{RT}\right] \text{ (Equation 8)}$$

The parameters in the equation, such as A_j and E_j, were determined from the experimental results as shown in Table 3. Moreover, when the ACTIVE substance is converted to CHAR and GAS, the char formation mass ratios are 0.35, 0.60, and 0.75 for cellulose, hemicellulose, and lignin, respectively.

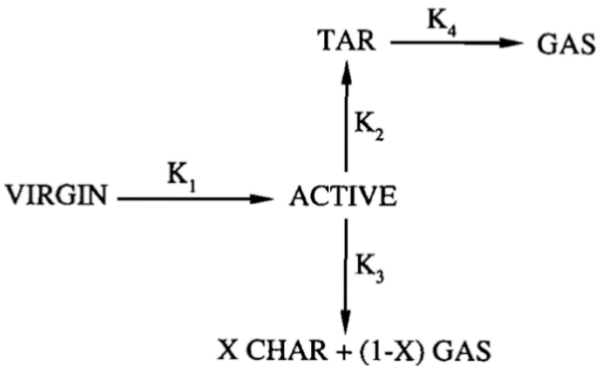

Figure 16: Reaction Model [58]

Table 3: Components Reduction Parameters [58]

Reactio	$A_j[1/s]$	$E_j[KJ/mol]$	Source
k_1^c	2.8×10^{19}	242.4	Di Blasi and Russo (1994)
k_2^c	3.28×10^{14}	196.5	Di Blasi and Russo (1994)
k_3^c	1.3×10^{10}	150.5	Di Blasi and Russo (1994)
k_1^h	2.1×10^{16}	186.7	Ward & braslaw (1985)*
k_2^h	8.75×10^{15}	202.4	Di Blasi and Russo (1994)*
k_3^h	2.6×10^{11}	145.7	Di Blasi and Russo (1994)*
k_1^l	9.6×10^{8}	107.6	Ward & braslaw (1985)*
k_2^l	1.5×10^{9}	143.8	Koufopanos et al. (1989)*
k_3^l	7.7×10^{6}	111.4	Koufopanos et al. (1989)*
k_4	4.28×10^{6}	108.0	Di Blasi and Russo (1994)

2.2 **The Comparison between the Experimental and the Calculation Results**

To evaluate the reproducibility of the overall kinetic model, the comparison between the experimental results and the theoretical results using the general kinetic model was carried out. The values for the parameters were used in Table 3, and the TG and the DTG curves were calculated.

To validate the experimental results, a Python code was utilized that could generate graphs based on the model proposed by Miller [58] and the kinetic parameters for the horse manure. The code may be referred to in the appendices section.

It is essential to predict the mass variation and the heat amount for manure during pyrolysis in order to evaluate the characteristics of the waste. In the 2nd part, the calculation for the mass variation during pyrolysis was attempted in the first modeling step. At first, using the overall kinetic reaction parameters and the Arrhenius equation, the comparison between the experimental and the theoretical results was carried out. Then, using the analytical model proposed by Miller, the comparison between the experimental and the theoretical results and the availability of the analytical model were evaluated. In this case, the estimate of the composition of the manure was done using the mass variation per unit time. Then, the mass variation per unit of time was obtained from the experimental results using the following equation:

$$\alpha = \frac{w_0 - W_t}{w_0 - w_f} = \frac{v_t}{v_f} \quad \text{(Equation 1)}$$

$$\frac{d\alpha}{dt} = \frac{(\alpha_t - \alpha_{t-1})}{\Delta t} \quad \text{(Equation 2)}$$

3. The Evaluation of the Composition

This code can be used for any animal manure or all types of waste, whereas the numerical results cannot factor in the effects of the impurities. However, the theoretical results are similar to the experimental results. Figure 17 is the graph for the experimental results for three different heating rates. Three random heating rates were picked 5°C/min, 20°C/min, and 35°C/min, and their trends from Figure 13 are compared in a new graph with a theoretically generated graph. Figure 18 is the graph for the theoretical results using the Miller model and the code to generate the curves for the same mass and heating rates. It can be noted that the curves in both graphs follow the same trend, which could be used to validate experimental data. As explained previously in the results, the peaks represent the cellulosic bonds, including hemicellulose and cellulose bonds, which occur in both experimental and theoretical graphs. The theoretical graph is clearer because it does not involve any moisture evaporation nor include any impurities in the sample.

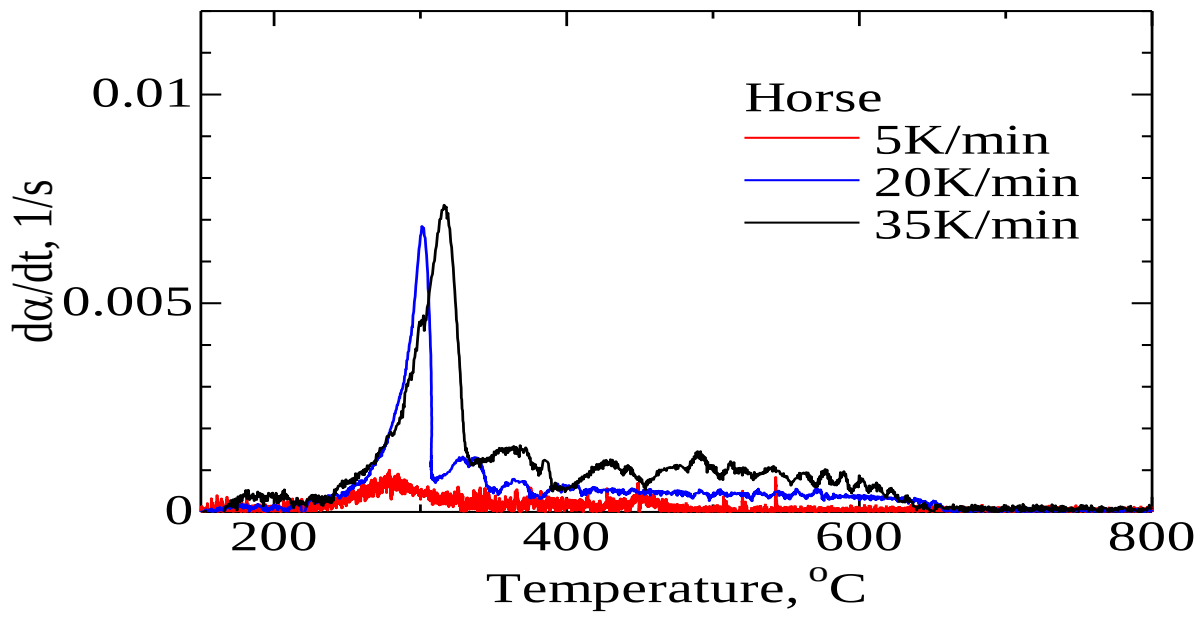

Figure 17: The Experimental Rate of Extent of Reaction for Horse Manure

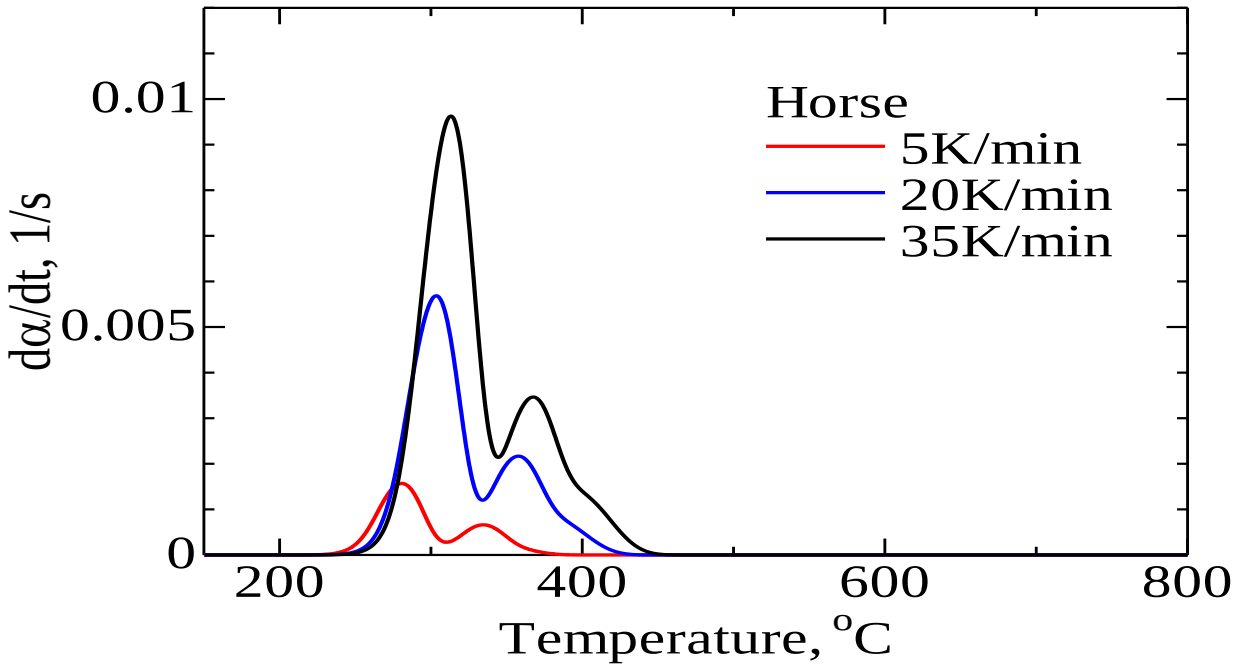

Figure 18: The Theoretical Rate of Extent of Reaction for Horse Manure

Chapter 5: Conclusion

This research study was done to investigate the effect of the heating rate on the temperature of the thermal cracking of the horse manure composition. The process used was pyrolysis, which used nitrogen as a gas agent and a temperature range between room temperature and up to 1,000°C. Eight different heating rates were used, which are 5°C/min, 10°C/min, 15°C/min, 20°C/min, 25°C/min, 30°C/min, 35°C/min, and 40°C/min. Increasing the heat rate in the pyrolysis process causes a latency in the reaction due to the lack of time to complete the reaction, which leads to a latency in the thermal degradation of the sample compositions: hemicellulose, cellulose, and lignin. Regarding endothermic and exothermic reactions, the most stable curves are 5, 10, and 15°C/minute. However, the most self-sustainable heating rate is 5° C/min, which allows enough time for the reaction to be completed. The slowest heating rates allow enough time for a complete reaction and do not cause latency in peaks and higher spikes; rather they provide gradually increases in energy. However, these slow processes use more energy in the furnace because they have a longer operating time to achieve a similar amount of energy. For example, by doubling the rate of 5°C to 10°C, the running time is reduced by half. From the graphs, small peaks in higher temperature represent the mass degradation due to the lignin composition. The horse manure consists of a higher percentage of hemicellulose and cellulose and a significantly smaller amount of lignin. Moreover, data from the horse pyrolysis is compared to different types of manure which are sheep, cow, chicken manure, which are to be mixed for a more self-sustainable energy generation using biomass. The goal of this comparison is to find the optimal combination of manure in order to achieve a more stable and sustainable energy. Energy is released as a result of the thermal cracking of biomass chemical compositions due to the adequate amount of heat applied. Different types of animal manure require distinct temperatures for the bonds of the compounds to break down into more simple chemical

molecules known as syngas. For instance, horse manure requires a relatively low amount of heat for the cellulosic thermal cracking to be achieved. Horse manure consists of a negligible amount of lignin, which means all the energy from horse manure is released from the thermal cracking of cellulosic bonds. On the other hand, cow manure requires applying higher heat for cellulosic thermal cracking. Therefore, by mixing horse manure with cow manure, mass degradation will occur at a wider range of temperature. This means that thermal cracking for cellulose for one animal requires a certain temperature that is different than the temperature required by cellulose in a different type of animal. Potential for higher energy continuity is achieved by combining the different animal manure types and linked to the different thermal cracking temperatures for lignocellulosic bonding. The combination could be between horse and sheep, horse and cow, chicken and sheep, etc. The experimental results for the thermal degradation of the cellulose and hemicellulose are validated using the mathematic model from Miller et al., which was used to develop a code that could be used to predict the mass and heat analysis for the pyrolysis process with different parameters and different organic animals.

Chapter 6: Challenges and Future Work

Future work and plan for improvement

This study will be more profound for future work as time will allow for more focus and resources. First, we would move forward with a co-pyrolysis process, in which more than one type of manure will be mixed. According to Figure 17, a more sustainable steady energy is developed by combining horse with either cow or sheep manure, as their thermal bonding cracking occurs at different temperatures. When the horse manure moves toward an endothermic reaction, sheep manure starts an exothermic reaction, which keeps the energy generation for a longer range of time. Second, gasification will be investigated using compressed air because this process is faster. Third, a comparison is to be done between the two processes and different types of feedstocks. For the most economically efficient process of converting biomass into clean, renewable energy, a study will be done using other processes that combine several types of feedstocks along with the possibility of adding a catalyst for a faster reaction. Finally, we would do a gas analysis using gas chromatography available at the university's chemistry lab.

Mistakes that were made will be corrected and improved upon. One of the improvements would be to avoid running experiments back-to-back sequentially but rather on different days or where enough time is provided for a device to cool down to the ambient temperature. Also, when the device is overused and more load is applied to the device, fluctuations appear in the results. One particularly important factor to improve upon is the consistency of mass; whereas in this study, the mass was not constant but varied for all runs. The results show a different magnitude in the y-axis for other runs due to the mass load variety.

Challenges faced

The device DTG from Shimadzu was shared among more than six users simultaneously. This had many disadvantages. First, to use it, it had to be reserved ahead of time for weekday hours. The experiments for this study were mostly performed after working hours during weekdays or during the weekend when the lab was less occupied. Second, because the device had several users, it also had more load. Also, these different users conducted their experiments with different setups and different types of samples that required more frequent maintenance. As mentioned in the experimental setup in chapter 3, the device takes up to or possibly more than 60 days to calibrate. Our experiment had to stop more than once for recalibration before it was discontinued. The main issue is failure to provide accurate data for heat analysis and shows no exothermic reaction. The device has not yet been repaired since May 2022.

Therefore, Professor Amano had to proceed with constructing a new lab for biomass and started searching for an ultimate lab setup that met our needs and expectations for more successful research. After a long search on the internet and multiple quotes, the decision was made to select the Simultaneous Therma Analyzer SDT 650 from TA Instruments, shown in Figure 19, against similar devices from Shimazu and METTLER TOLEDO. The decision was based on many factors, such as cost, maintenance, technical support, accessibility and usage, and software updates.

First, the TA Instruments has more effective and rapid technical support, available locally, compared to Toledo and Shimadzu, the two other companies whose technicians are based out of state. Second, the software from TA Instruments, TRIOS, has a more friendly user interface and more functionality to control the gases and their flow rates, the input setup, and the heat rates, especially for providing more output options. These options in output could be selected from wattage or voltage for heat change; it also includes enthalpy change and many more selections. Third, for the device's

maintenance prevention. Two options prevent the most common failures in this category of devices: the damage of the thermal sensor due to the lower flow rate of the purging gas responsible for cooling the device from overheating, and the damage to the rods where the mass analysis sensor was rendered inaccurate due to unwanted pressure while loading or discharging the sample. Their solution was housed in the software where the experiment is not allowed to start unless adequate gas pressure is available. The solution for the rod sensitivity is placing a metal arm support beneath the sample holder to take up any unwanted pressure the user applies during the sample loading.

Figure 19: SDT 650 from TA Instruments

References

[1] *Frequently asked questions (faqs) - U.S. energy information administration (EIA)*. Frequently Asked Questions (FAQs) - U.S. Energy Information Administration (EIA). (n.d.). FAQs

[2] "U.S. Energy Information Administration - EIA - Independent Statistics and Analysis." *U.S. Energy Facts Explained - Consumption and Production - U.S. Energy Information Administration (EIA)*, FAQs. Accessed 15 Oct. 2023.

[3] "U.S. Energy Information Administration - EIA - Independent Statistics and Analysis." *Biomass Explained - U.S. Energy Information Administration (EIA)*, www.eia.gov/energyexplained/biomass/. Accessed 15 Oct. 2023.

[4] "Biomass Energy." *Education*, education.nationalgeographic.org/resource/biomass-energy/. Accessed 15 Oct. 2023.

[5] *Top Five reasons to compost*. Top five reasons to compost - ACSWMD. (n.d.). https://www.addisoncountyrecycles.org/food-scraps/composting/101/why-compost

[6] Environmental and Energy Study Institute (EESI). "Fact Sheet: Biogas: Converting Waste to Energy." *EESI*, www.eesi.org/papers/view/fact-sheet-biogasconverting-waste-to-energy. Accessed 15 Oct. 2023.

[7] *Greenhouse effect*. Education. (n.d.). https://education.nationalgeographic.org/resource/greenhouse-effect/

[8] *Climate change: The greenhouse gases causing global warming: News: European parliament*. Climate change: the greenhouse gases causing global warming | News | European Parliament. (2023, March 23). FAQs

[9] Denchak, Melissa. "Greenhouse Effect 101." *Be a Force for the Future*, 5 June 2023, www.nrdc.org/stories/greenhouse-effect-101#gases.

[10] Biomass as feedstock for a bioenergy and bioproducts industry: The ... (n.d.-a). https://www.energy.gov/eere/bioenergy/articles/biomass-feedstock-bioenergy-and-bioproducts-industry-technical-feasibility

[11] ELSAYED, OSAMA Mansour Selim, "Enhancement of Energy Efficiency for Thermal Energy and Biomass Driven Applications" (2022). Theses and Dissertations. 2884. https://dc.uwm.edu/etd/2884

[12] (6254140f4ceaa), Mary Quaney. ""The Global Geopolitical Risks Arising from Fossil Fuel Reliance Are No Longer Sustainable."" *Recharge*, 11 Apr. 2022,

www.rechargenews.com/energy-transition/the-global-geopolitical-risks-arising-from-fossil-fuel-reliance-are-no-longer-sustainable/2-1-1200734.

[13] "Fossil Fuels." *ELI: Energy: Support Materials: Fossil Fuels*, ei.lehigh.edu/learners/energy/fossilfuels/fossilfuels11.html#:~:text=Despite%20their%20negative%20environmental%20impacts,and%20sometimes%E2%80%94around%20the%20world.&text=Petroleum%20(crude%20oil)%20is%20relatively,cause%20catastrophic%20damage%20if%20spilled.

[14] Kumar, A., Jones, D., & Hanna, M. (2009). Thermochemical biomass gasification: A review of the current status of the technology. *Energies*, *2*(3), 556–581. https://doi.org/10.3390/en20300556

[15] Biological manipulation of manure: Getting what you want from animal. Penn State extension. (n.d.). https://extension.psu.edu/biological-manipulation-of-manure-getting-what-you-want-from-animal-manure

[16] Bentsen, N. S., Felby, C., & Thorsen, B. J. (2014). Agricultural Residue Production and potentials for energy and Materials Services. *Progress in Energy and Combustion Science*, *40*, 59–73. https://doi.org/10.1016/j.pecs.2013.09.003

[17] Turning agricultural residues and manure into Bioenergy. (n.d.). https://www.canr.msu.edu/uploads/files/Agricultural-Residue-Ranking.pdf

[18] "Biomass Resources." *Energy.Gov*, www.energy.gov/eere/bioenergy/biomass-resources.

[19] Facts and figures about materials, waste and recycling. (n.d.-b). https://www.epa.gov/facts-and-figures-about-materials-waste-and-recycling

[20] The sources and solutions: Wastewater | US EPA. (n.d.-c). https://www.epa.gov/nutrientpollution/sources-and-solutions-wastewater

[21] Marc@renergon. (2022, September 5). *Anaerobic digestion explained*. RENERGON. https://www.renergon-biogas.com/en/anaerobic-digestion-explained/

[22] *Incineration of sludge*. Sludge Processing. (n.d.). https://www.sludgeprocessing.com/oxidative-thermochemical-treatment/incineration-sludge/

[23] Animal Feeding Operations - uses of Manure | US EPA. (n.d.). https://www.epa.gov/npdes/animal-feeding-operations-uses-manure

[24] Lead Author Lead Author: Mary A. Keena Extension Specialist/Livestock Environmental Management Carrington Research Extension Center, & Lead Author: Mary A. Keena Extension Specialist/Livestock Environmental Management Carrington Research Extension Center. (2022, March 4). *Composting animal manures: A guide to the process and*

management of animal manure compost. NDSU Agriculture. https://www.ndsu.edu/agriculture/extension/publications/composting-animal-manures-guide-process-and-management-animal-manure-compost

[25] *United States Department of Agriculture*. USDA. (n.d.). https://www.nass.usda.gov/Publications/AgCensus/2017/Full_Report/Volume_1,_Chapter_1_US/

[26] Hussein, M.S., Burra, K.G., Amano, R.S., and Gupta, A.K., "Effect of oxygen addition in steam gasification of chicken manure," ***Fuel (IF=5.2),*** Vol. 189, Feb. 2017, 189, Pp 428-435, IF=3.6. https://doi.org/10.1016/j.fuel.2016.11.005

[27] admin, L. (2020, September 4). *Liquid manure storage ponds, pits, and tanks*. Livestock and Poultry Environmental Learning Community. https://lpelc.org/liquid-manure-storage-ponds-pits-and-tanks/

[28] Hoffman, B. (2014, May 14). *What the pork? China, pigs and poop*. Forbes. https://www.forbes.com/sites/bethhoffman/2014/05/13/what-the-pork-china-pigs-and-poop/?sh=278925e24d17

[29] Lundgren, J., & Pettersson, E. (2009). Combustion of horse manure for heat production. *Bioresource Technology*, *100*(12), 3121–3126. https://doi.org/10.1016/j.biortech.2009.01.05 0

[30] Da Lio, L., Castello, P., Gianfelice, G., Cavalli, R., & Canu, P. (2021). Effective energy exploitation from horse manure combustion. *Waste Management*, *128*, 243–250. https://doi.org/10.1016/j.wasman.2021.04.035

[31] Cui, Z., Shi, J., & Li, Y. (2011). Solid-state anaerobic digestion of spent wheat straw from horse stall. *Bioresource Technology*, *102*(20), 9432–9437.https://doi.org/10.1016/j.biortech.2011.07.062

[32] Manure as fuel. (n.d.). http://large.stanford.edu/courses/2010/ph240/birer1/

[33] *Fossil fuels*. ELI: Energy: Support Materials: Fossil Fuels. (n.d.). https://ei.lehigh.edu/learners/energy/fossilfuels/fossilfuels11.html#:~:text=Despite%20their%20negative%20environmental%20impacts,and%20sometimes—around%20the%20world.&text=Petroleum%20(crude%20oil)%20is%20relatively,cause%20catastrophic%20damage%20if%20spilled

[34] *EIA projects nearly 50% increase in world energy usage by 2050, led by growth in Asia*. Homepage - U.S. Energy Information Administration (EIA). (n.d.). https://www.eia.gov/todayinenergy/detail.php?id=41433#:~:text=In%20its%20newly%20released%20International,50%25%20between%202018%20and%202050.

[35] Brethauer, S., & Studer, M. H. (2015). Biochemical conversion processes of lignocellulosic biomass to fuels and chemicals – A Review. *CHIMIA*, *69*(10), 572. https://doi.org/10.2533/chimia.2015.572

[36] CITESEERX. (n.d.-b). https://citeseerx.ist.psu.edu/document?repid=rep1&type=pdf&doi=afa0bad9602fbf152011c2c88cd67ad209446b22

[37] Khalid, A., Arshad, M., Anjum, M., Mahmood, T., & Dawson, L. (2011). The anaerobic digestion of solid organic waste. *Waste Management*, *31*(8), 1737–1744. https://doi.org/10.1016/j.wasman.2011.03.021

[38] Stuart, Peter. "The advantages and disadvantages of anaerobic digestion as a renewable energy source." *Loughborough University, Loughborough* (2006).

[39] Evangelisti, C., Bossola, F., & Dal Santo, V. (2017). Catalysts for hydrogen production from renewable raw materials, byproducts and waste. *Hydrogen Production, Separation and Purification for Energy*, 71–101. https://doi.org/10.1049/pbpo089e_ch3

[40] Knothe, G., Krahl, J., & Gerpen, J. V. (2015). *The biodiesel handbook*. Elsevier Science.

[41] Amano, R.S. and Hussein, M.S.I., "Study of Biofuel Animal Manure," Innovations in Sustainable Energy and Cleaner Environment, pp 529-539, Green Energy and Technology book series (GREEN), 2020 Springer Nature Switzerland AG, ISBN 978-981-13-9011-1 ISBN 978-981-13-9012-8 (eBook)

[42] Kumar, A., Jones, D., & Hanna, M. (2009a). Thermochemical biomass gasification: A review of the current status of the technology. *Energies*, *2*(3), 556–581. https://doi.org/10.3390/en20300556

[43] Mallick, D., Buragohain, B., Mahanta, P., & Moholkar, V. S. (2017). Gasification of mixed biomass: Analysis using equilibrium, semi-equilibrium, and kinetic models. *Coal and* Biomass Gasification, 223–241. https://doi.org/10.1007/978-981-10-7335-9_9

[44] Hussein, M.S., Burra, K.R., Amano, R.S., and Gupta, A.K, "Temperature and Gasifying Media Effects on Chicken Manure Pyrolysis and Gasification," ***Fuel (IF=5.2),*** Vol. 202, August 2017, pp. 36-45. https://doi.org/10.1016/j.fuel.2017.04.017

[45] Amano, R.S. and Hussein, M.S., "Simultaneous Differential Thermal and Thermogravimetric Analysis of Chicken Manure Gasification using Nitrogen and Carbon Dioxide," 2016 AIAA Propulsion and Energy, July 25-27, 2016, Salt Lake City, Utah

[46] Amano, Ryoichi, Mohamed Ibrahim, and Alka Gupta, 2013, "Experimental Investigation of Gasification of Biomass Using Carbon Dioxide." *51st AIAA Aerospace Sciences Meeting*, including the New Horizons Forum and Aerospace Exposition.

[47] Burra, K.R., Hussein, M.S., Amano, R.S., and Gupta, A.K, "Syngas Evolutionary Behavior during Chicken Manure Pyrolysis and Air Gasification," Applied Energy (IF=8.5), Vol. 181, November 2017, pp. 408-415, https://doi.org/10.1016/j.apenergy.2016.08.095_

[48] Trninic, M., Stojiljkovic, D., Jovovic, A., & Jankes, G. (2016). Biomass gasification technology: The state of the art overview. *2016 4th International Symposium on Environmental Friendly Energies and Applications (EFEA)*. https://doi.org/10.1109/efea.2016.7748797

[49] Fernandez-Lopez, M., Pedrosa-Castro, G. J., Valverde, J. L., & Sanchez-Silva, L. (2016). Kinetic analysis of manure pyrolysis and Combustion Processes. *Waste Management*, *58*, 230–240. https://doi.org/10.1016/j.wasman.2016.08.027

[50] Selim, O. M., & Amano, R. S. (2020). Co-pyrolysis of chicken and cow manure. *Journal of Energy Resources Technology*, *143*(1). https://doi.org/10.1115/1.4047597

[51] Selim, O., Hussein, M., and Amano, R.S., "Effect of Heating Rate on Chemical Kinetics of Chicken Manure With Different Gas Agents," Trans. ASME J. Energy Resources Technology (IF=3.183), Oct 2020, 142(10): 102104 (7 pages), https://doi.org/10.1115/1.4047018

[52] Posted By Equine Science Center at 1:54 am. (n.d.). *Horses and manure*. Equine Science Center. https://esc.rutgers.edu/fact_sheet/horses-and-manure/

[53] Zongliu. (2017, July 27). Manure to Energy: Understanding Processes, principles and Jargon. Texas Animal Manure Management Issues. https://tammi.tamu.edu/2017/07/17/manure-energy-understanding-processes-principles-jargon/

[54] *Understanding a hay analysis*. Penn State Extension. (n.d.-b). https://extension.psu.edu/understanding-a-hay-analysis

[55] Shimadzu 2021, DTG-60A DTG-60AH Instruction Manual, SHIMADZU AUTO SIMULTANEOUS MEASUREMENTS OF THERMOGRAVIMETRY AND DIFFERENTIAL THERMAL ANALYSIS. https://www.shimadzu.com

[56] Selim, O. M., Maache, M., Kada, C., Kumano, H., & Amano, R. (2023). Thermochemical conversion of cow manure with different heating rates. *ASME Power Applied R&D 2023*. https://doi.org/10.1115/power2023-108750

[57] Biomass Energy. Education. (n.d.). https://education.nationalgeographic.org/resource/biomass-energy/

[58] R.S. Miller, J. Bellan, A Generalized Biomass Pyrolysis Model Based on Superimposed Cellulose, Hemicellulose and Lignin Kinetics, Combustion Science and Technology, 1997, 126, 97-137

APPENDIX A: FIGURES FOR GLOBAL AND REGEONAL STATISTICAL CHARTS ABOUT ENERGY AND RESOURCES.

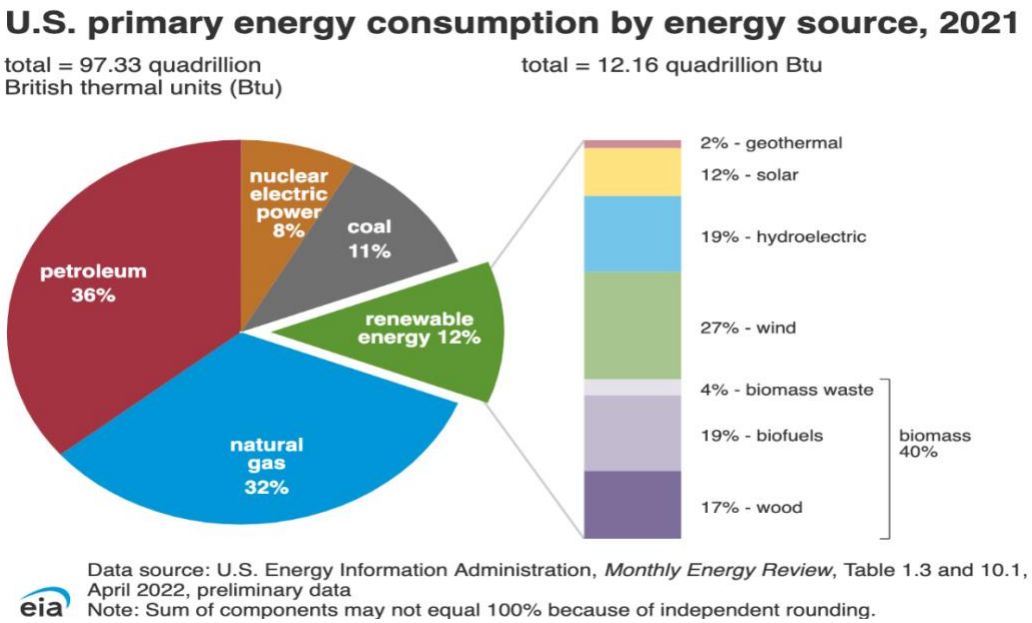

Figure A1: U.S. primary energy consumption by energy source, 2021

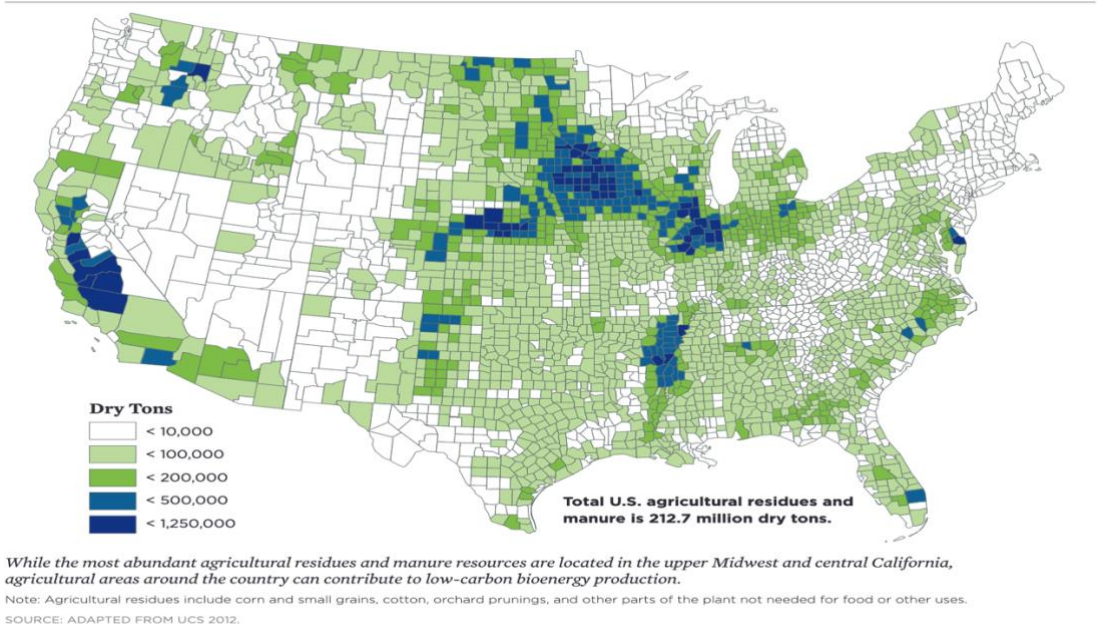

Figure A2: Agricultural Residues and Manure Availability Projection in 2030

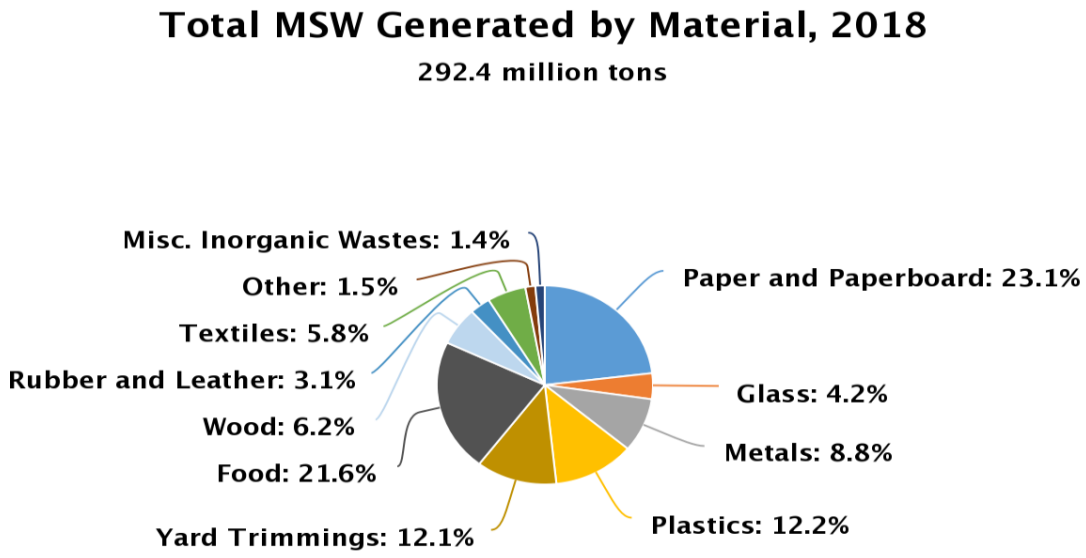

Figure A3: Total Municipal Solid Waste Generated by Material in the US, 2018

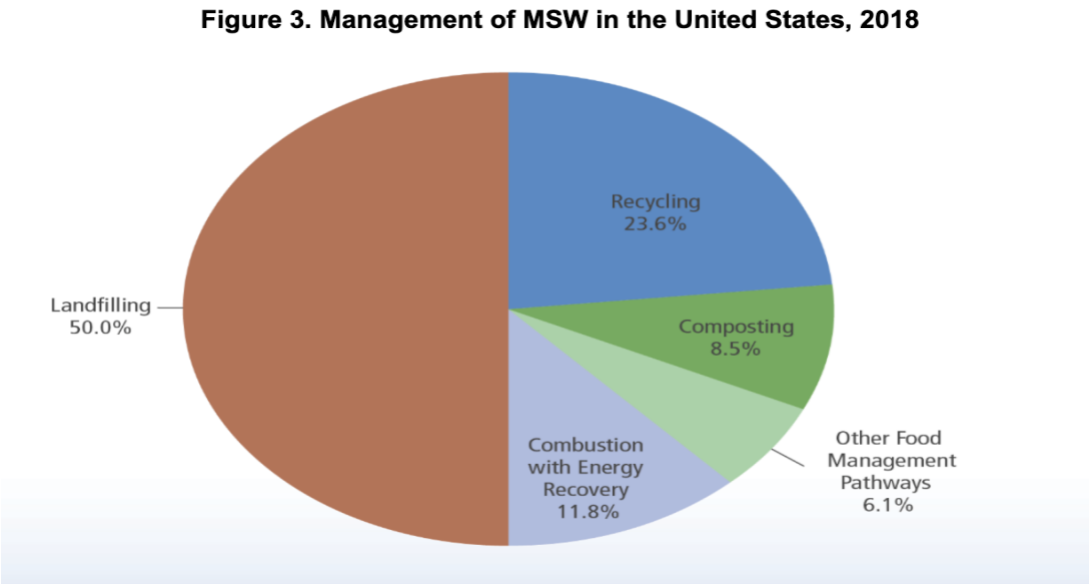

Figure A4: Management of Municipal Solid Waste in the US, 2018

APPENDIX B: FIGURES FOR PROCEDURE AND METHODOLOGY

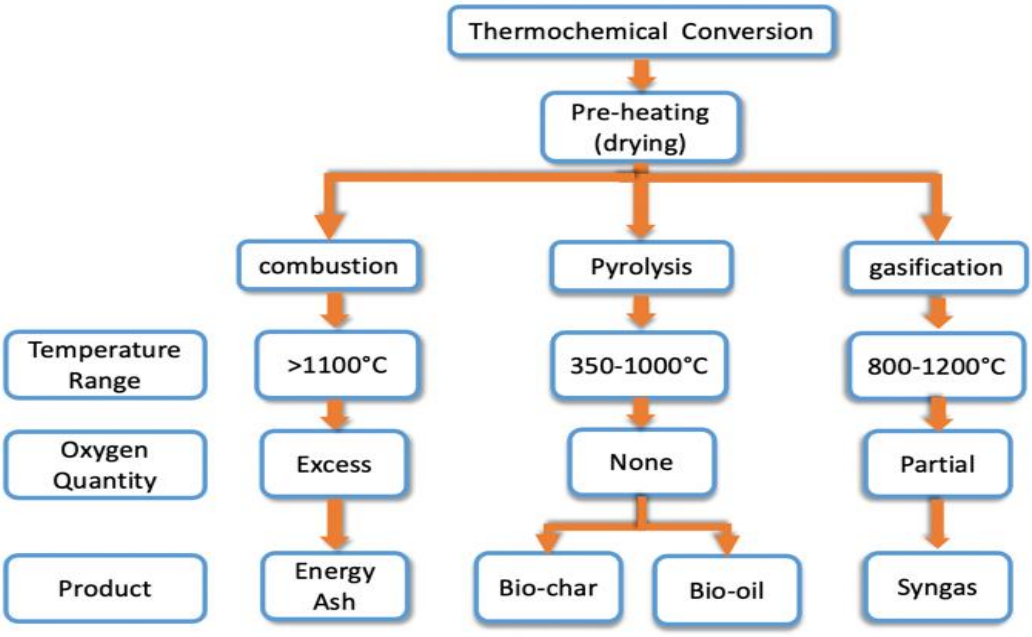

Figure B1: Diagram of the Thermochemical Conversion Processes

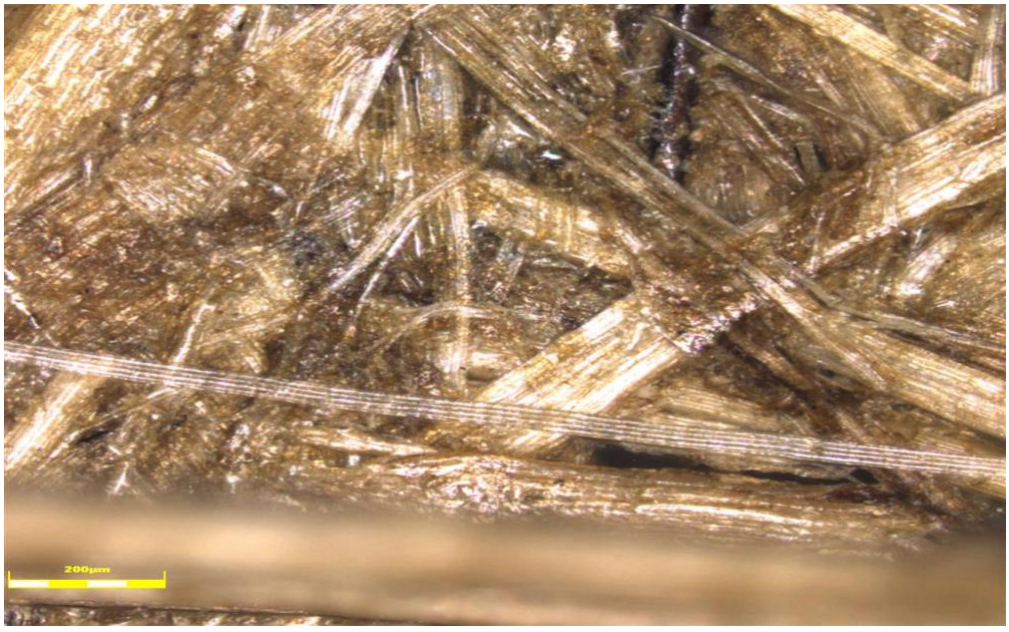

Figure B2: microscopic image for horse manure at 200um scale

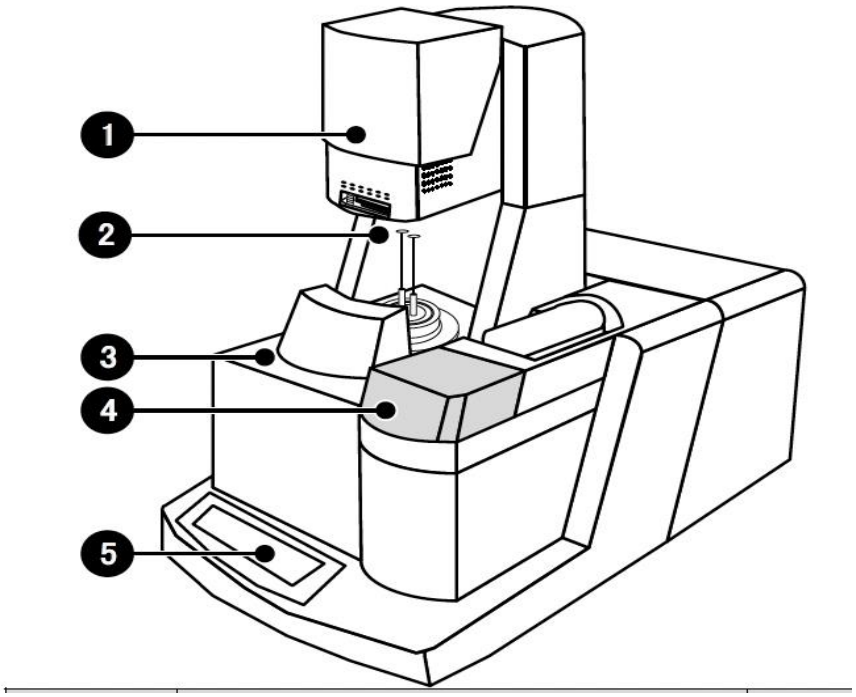

Figure B3: DTG 60 AH Components

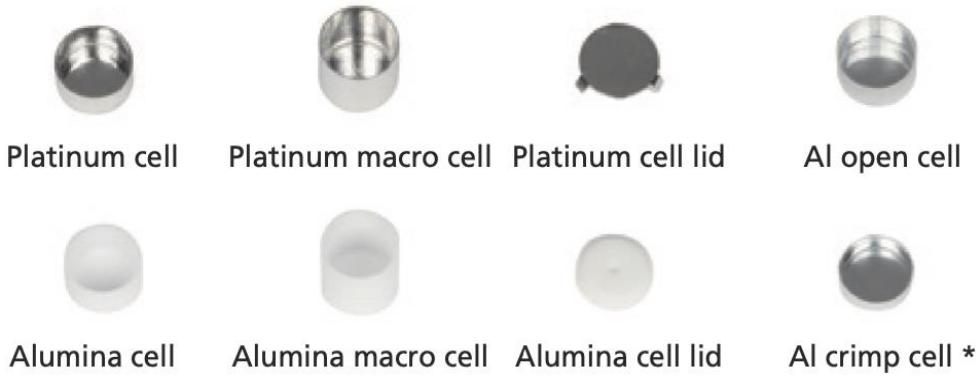

Figure B4: DTG Cells (Pans) Types

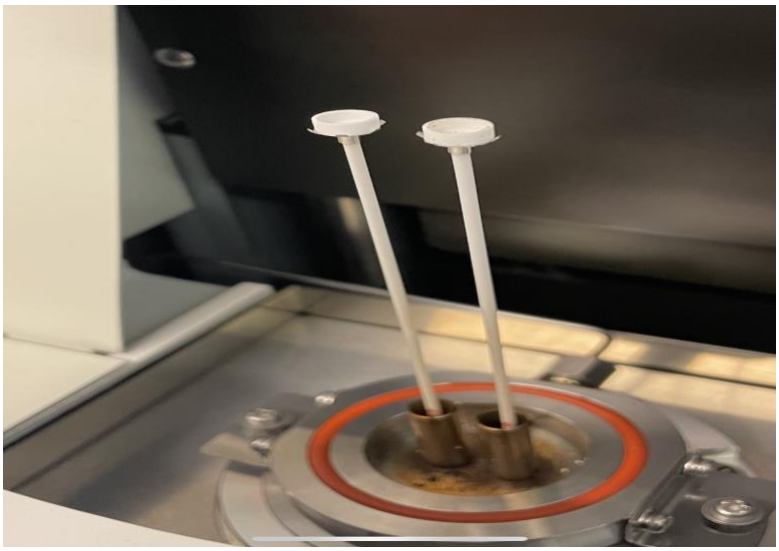

Figure B5: Thermocouples Sensors and Balance Rods

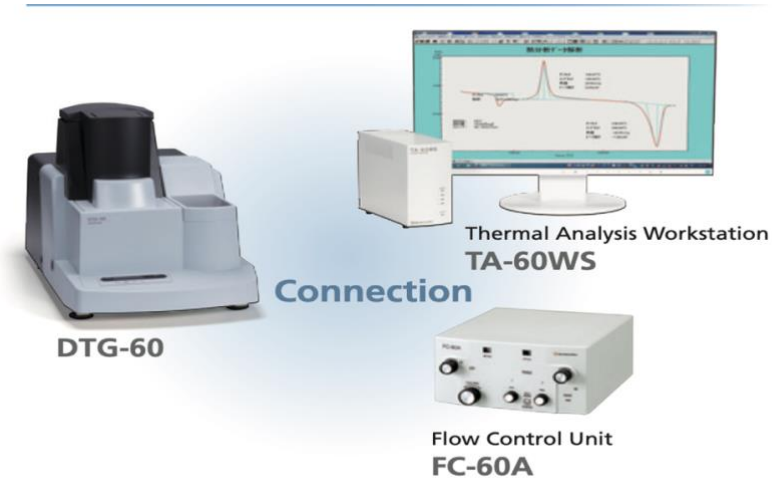

Figure B6: Apparatus Configuration

Figure B7: DTG-60AH From Shimadzu in The Global Water Center UWM

APPENDIX C: FIGURES FOR THE EXPERIMENTAL RESULTS

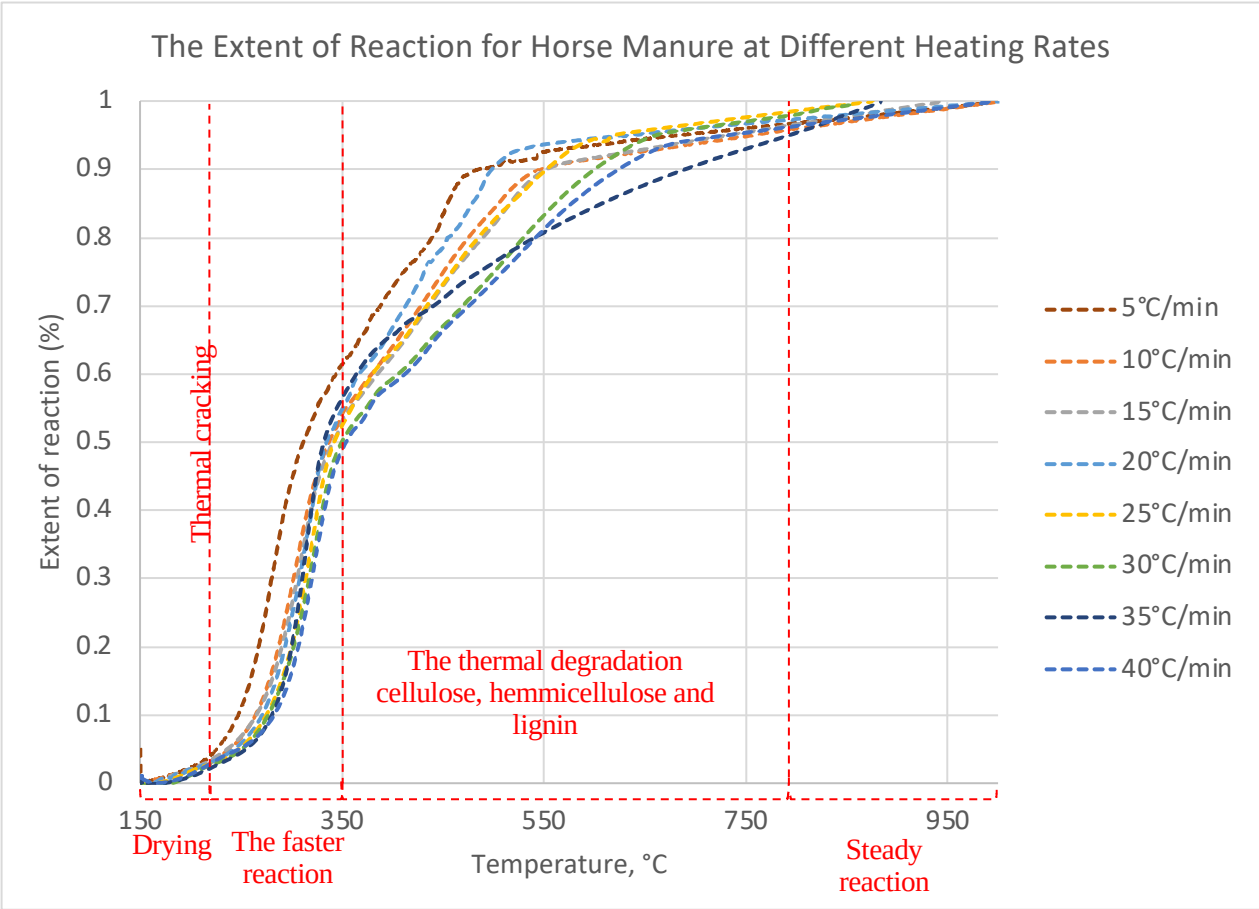

Figure C1: The Extent of Reaction vs. Temperature for Horse Manure at Different Heating Rates

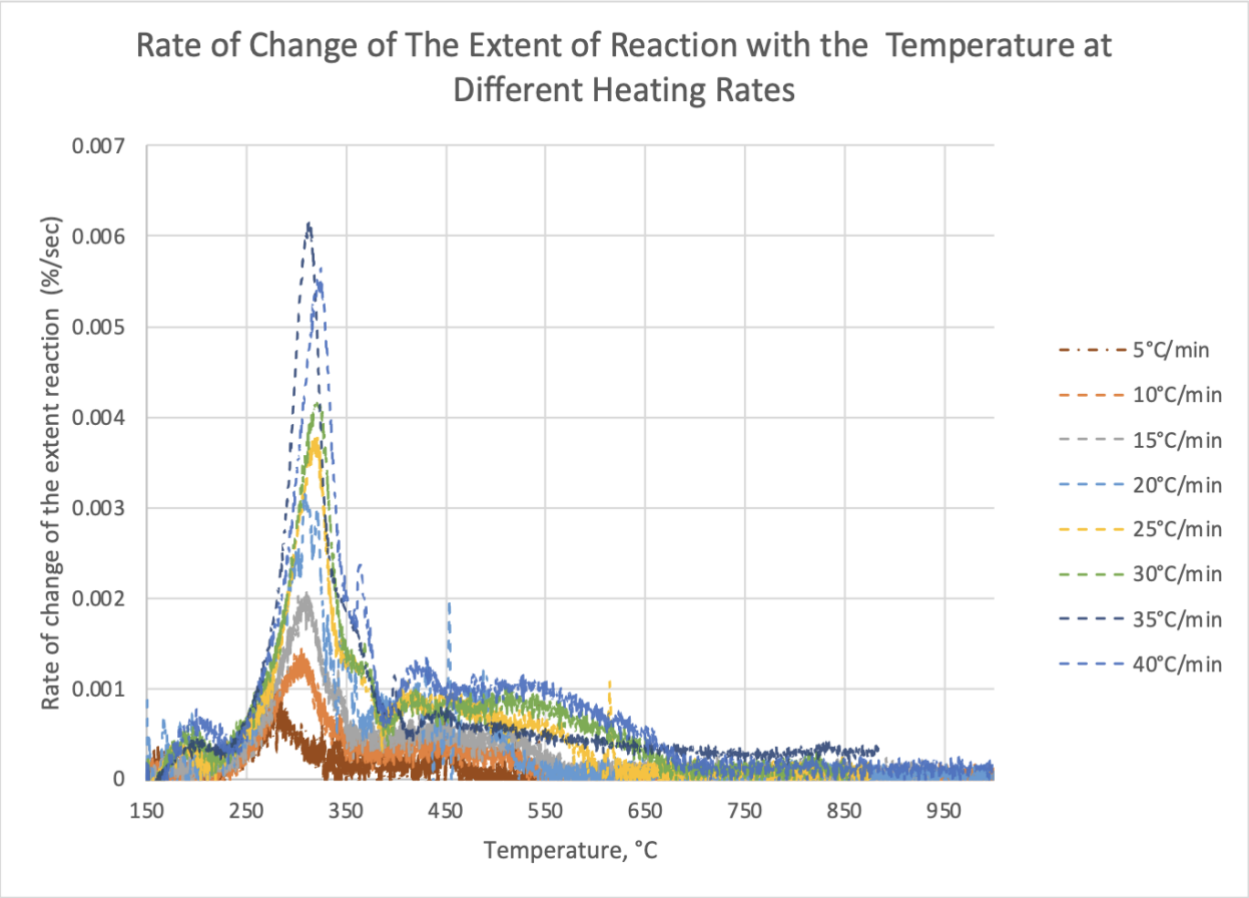

Figure C2: The Rate of The Extent of Reaction vs. Temperature at Different Heating Rates

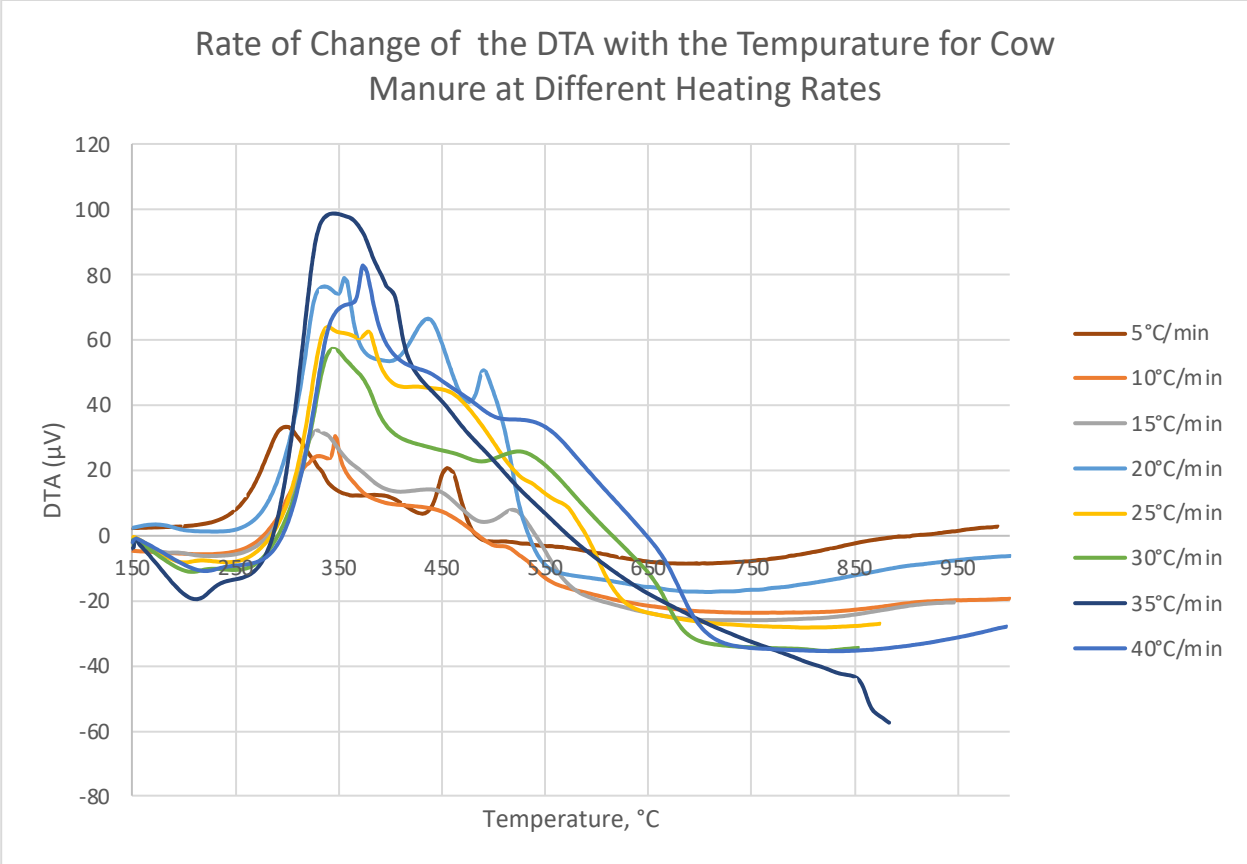

Figure C3: The Rate of DTA vs. Temperature for Cow Manure at Different Heating Rates

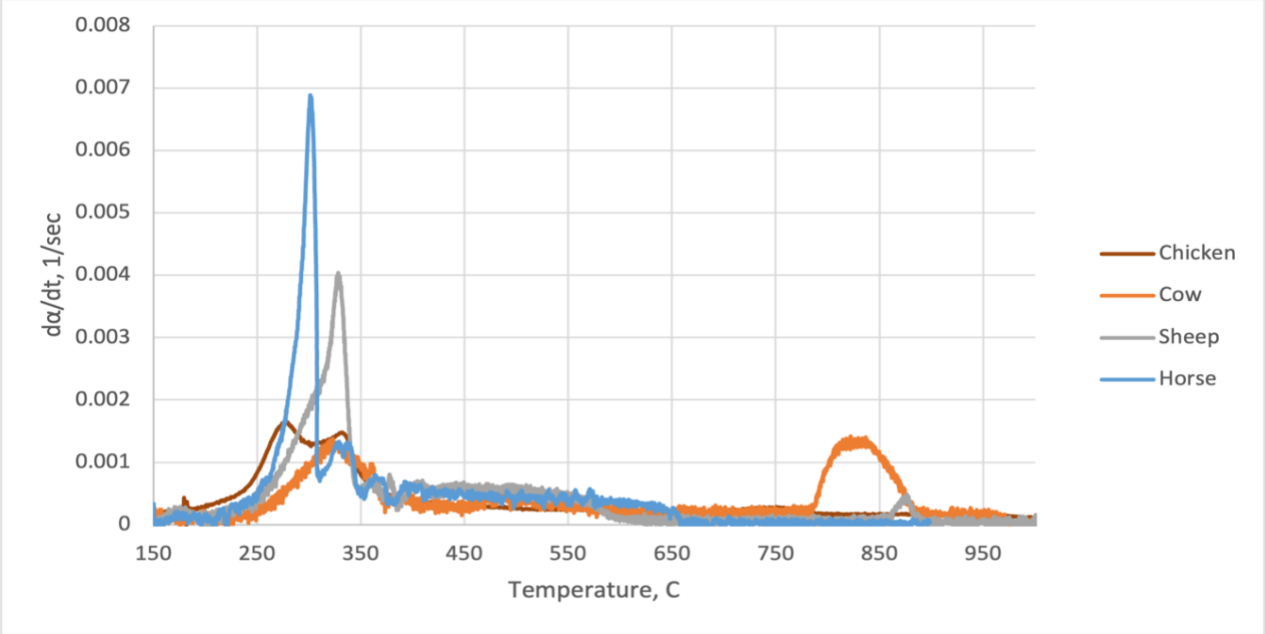

Figure C4: The Rate of DTA vs. Temperature for Cow Manure at Different Heating Rates

APPENDIX D: EXPERIMENTAL VALIDATION USING THEORETICAL MODLE

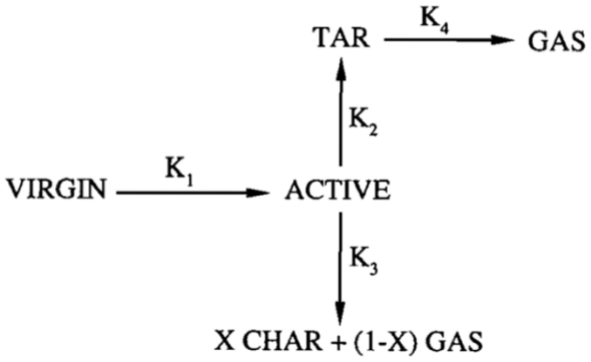

Figure D1: Reaction Model Diagram

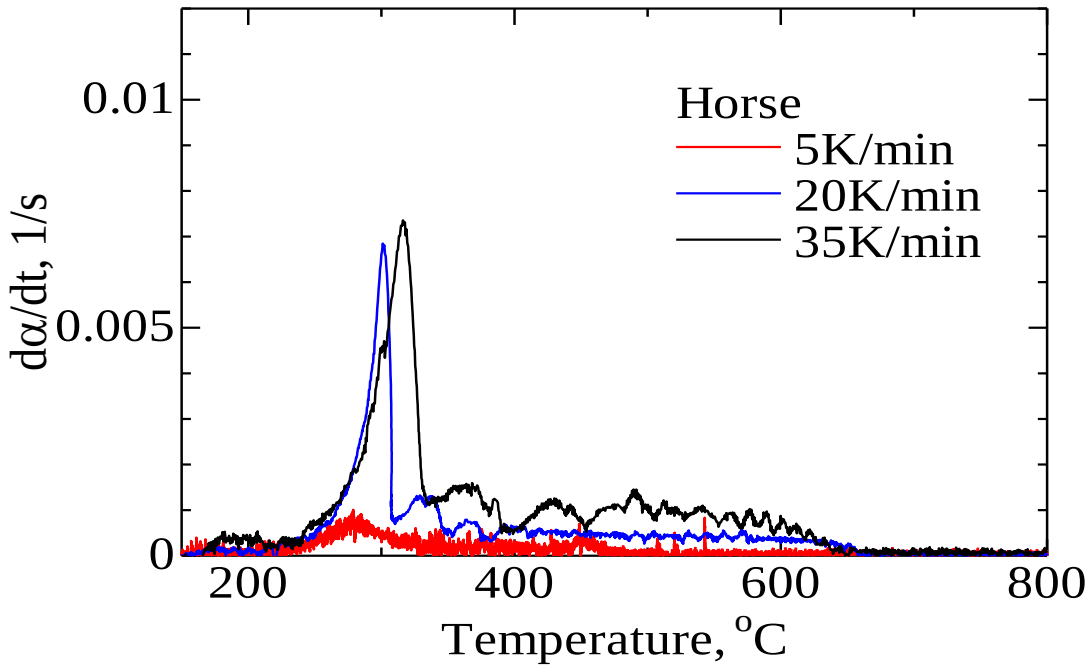

Figure D2: The Experimental Rate of Extent of Reaction for Horse Manure

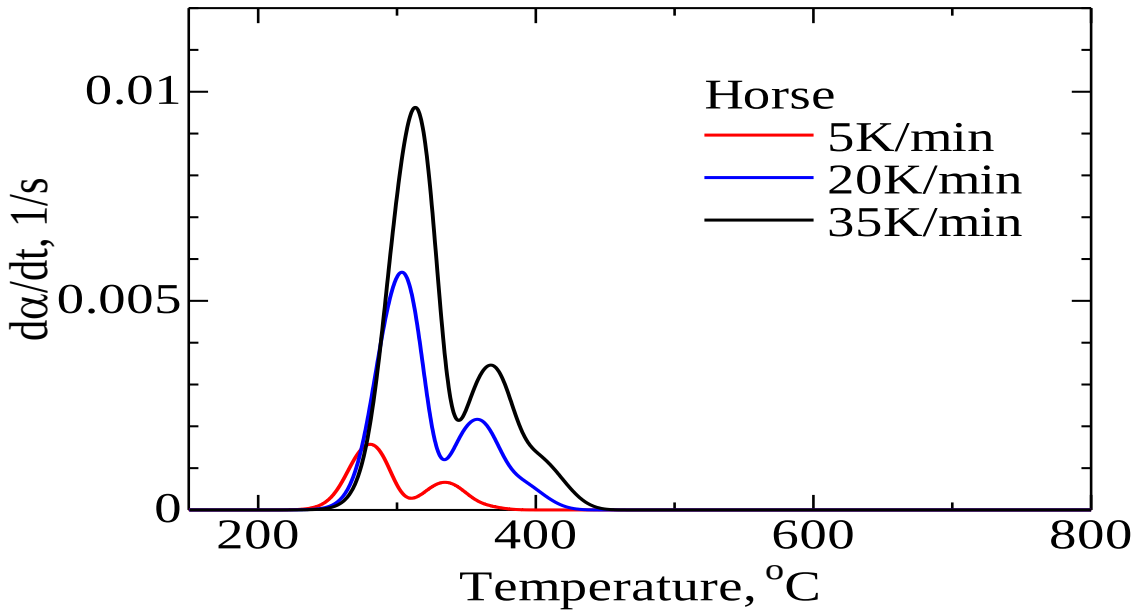

Figure D3 The Theoretical Rate of Extent of Reaction for Horse Manure

APPENDIX E: FIGURES FOR FUTURE WORK

Figure E1: SDT 650 from TA Instruments

APPENDIX F: TABLES

Table F1: Chemical Compositions for Dry Hay with Their Percentage of Availability

Term	Meaning	Typical Value
DM	Dry matter: The Nutrients without water	85%
Moisture	The amount of water in hay	11-16%
CP	Crude protein: the amount of protein in Hay	8-20%
ADF	Acid detergent fiber (cellulose + lignin): a measurement of fiber	30-45%
NDF	Neutral detergent fiber (hemicellulose + cellulose + lignin): a measurement of fiber	40-65%
NSC	Non-structural carbohydrates: a measurement of simple sugar and starch. Subset of this include WSC, ESC, and NFC.	5-25%
DE	Digestible energy: the amount of energy digested and used by the horse	0.75-1.0 Mcal/lb

Table F2: DTG 60AH Parts and Components

No.	Name
1	Furnace cover
2	Detector and reference rods
3	Tray for setting sample pans
4	autosampler
5	Kay/display section

Table F3: Components Reduction Parameters

Reaction	$A_j[1/s]$	$E_j[KJ/mol]$	Source
k_1^c	2.8×10^{19}	242.4	Di Blasi and Russo (1994)
k_2^c	3.28×10^{14}	196.5	Di Blasi and Russo (1994)
k_3^c	1.3×10^{10}	150.5	Di Blasi and Russo (1994)
k_1^h	2.1×10^{16}	186.7	Ward & braslaw (1985)*
k_2^h	8.75×10^{15}	202.4	Di Blasi and Russo (1994)*
k_3^h	2.6×10^{11}	145.7	Di Blasi and Russo (1994)*
k_1^l	9.6×10^{8}	107.6	Ward & braslaw (1985)*
k_2^l	1.5×10^{9}	143.8	Koufopanos et al. (1989)*
k_3^l	7.7×10^{6}	111.4	Koufopanos et al. (1989)*
k_4	4.28×10^{6}	108.0	Di Blasi and Russo (1994)

APPENDIX G: EQUATIONS

$$\alpha = \frac{w_0 - W_t}{w_0 - w_f} = \frac{v_t}{v_f} \text{ (Equation 1)}$$

$$\frac{d\alpha}{dt} = \frac{(\alpha_t - \alpha_{t-1})}{\Delta t} \text{ (Equation 2)}$$

$$k(T) = A \exp\left(\frac{-E_a}{RT}\right) \text{ (Equation 3)}$$

$$\frac{d\alpha}{dT} = \frac{k(T)}{\beta} f(\alpha) = \frac{A}{\beta} \exp\left(\frac{-E_a}{RT}\right) f(\alpha) \text{ (Equation 4)}$$

$$\frac{d\alpha}{dT} = k(T)(1-\alpha)^n \text{ (Equation 5)}$$

$$\frac{d\alpha}{dT} = \frac{k(T)}{\beta} f(\alpha) = \frac{A}{\beta} \exp\left(\frac{-E_a}{RT}\right)(1-\alpha)^n \text{ (Equation 6)}$$

$$ln\left(\frac{\frac{d\alpha}{dT}}{(1-\alpha)^n}\right) = \ln\left(\frac{A}{\beta}\right) - \left(\frac{E_a}{RT}\right) \text{ (Equation 7)}$$

$$K_j = A_j \exp\left[\frac{-E_j}{RT}\right] \text{ (Equation 8)}$$

APPENDIX H: PROGRAMING CODE FOR THE THEORETICAL MODEL PART

```
# Biomass
# Mass variation calculation using Miller-Bellan model
#               H. Kumano
#
import math
import csv
#
def func(i:int, t:float, y:float) -> float:
   ai = a[i]
   ei = e[i]
   f = ai * math.exp(ei / rgas / abstemp) * y
   return f
#
def rung(i:int, t:float, y:float) -> float:
   k1 = dt * func(i, t, y)
   k2 = dt * func(i, t + 0.5*dt, y + 0.5*k1)
   k3 = dt * func(i, t + 0.5*dt, y + 0.5*k2)
   k4 = dt * func(i, t + dt, y + k3)
   r = (k1 + 2.0*(k2+k3) + k4) / dt / 6.0
   return r
#
# Read from conf.csv
#
f_conf = open("conf.csv", "r")
reader = csv.reader(f_conf)
csv_data = list(reader)
ini_temp = float(csv_data[0][1])
end_temp = float(csv_data[1][1])
time_const = float(csv_data[2][1])
heat_rate = float(csv_data[3][1])
mass_cel_ini = float(csv_data[4][1])
mass_hem_ini = float(csv_data[5][1])
mass_lig_ini = float(csv_data[6][1])
dt = float(csv_data[7][1])
output_int = float(csv_data[8][1])
res_final = float(csv_data[9][1])
f_conf.close()
#
rgas = 8.314
#
```

```
# 0:Cel -> A-Cel 1:A-Cel -> Tar 2:A-Cel -> Char+Volatiles
# 3:Hem -> A-Hem 4:A-Hem -> Tar 5:A-Hem -> Char+Volatiles
# 6:Lig -> A-Lig 7:A-Lig -> Tar 8:A-Lig -> Char+Volatiles
#
a = [0.0]*9
e = [0.0]*9
reac_rate = [0.0]*9
#
a[0] = 2.80e19
a[1] = 3.28e14
a[2] = 1.30e10
a[3] = 2.10e16
a[4] = 8.75e15
a[5] = 2.60e11
a[6] = 9.60e8
a[7] = 1.50e9
a[8] = 7.70e6
#
e[0] = -242400.
e[1] = -196500.
e[2] = -150500.
e[3] = -186700.
e[4] = -202400.
e[5] = -145700.
e[6] = -107600.
e[7] = -143800.
e[8] = -111400.
#
#  Char production rate
#
cpr_c = 0.35
cpr_h = 0.60
cpr_l = 0.75
#
#  Cellulose
#
mass_cel = mass_cel_ini
mass_acel = 0.0
mass_ctar = 0.0
mass_cchr = 0.0
mass_cvol = 0.0
#
#  Hemicellulose
#
```

```
mass_hem = mass_hem_ini
mass_ahem = 0.0
mass_htar = 0.0
mass_hchr = 0.0
mass_hvol = 0.0
#
#  Lignin
#
mass_lig = mass_lig_ini
mass_alig = 0.0
mass_ltar = 0.0
mass_lchr = 0.0
mass_lvol = 0.0
#
res_total_cel = mass_cel + mass_acel + mass_cchr
res_total_hem = mass_hem + mass_ahem + mass_hchr
res_total_lig = mass_lig + mass_alig + mass_lchr
res_total = res_total_cel + res_total_hem + res_total_lig
#
a_now = 0.
#
time = 0.
time_const = time_const * 60.
temp = ini_temp
abstemp = temp + 273.15
#
lstop = False
ltemp = False
#
ioutput = 0
ioutput_int = int(output_int/dt)
#
f_total = open('total.csv', 'w', newline='')
f_comp = open('comp.csv', 'w', newline='')
f_dmdt = open('dmdt.csv', 'w', newline='')
f_dadt = open('dadt.csv', 'w', newline='')
writer_total = csv.writer(f_total)
writer_comp = csv.writer(f_comp)
writer_dmdt = csv.writer(f_dmdt)
writer_dadt = csv.writer(f_dadt)
#
header_total = ['time(sec)', 'abstmp(K)', 'temp(C)', 'mass-t', 'a']
header_comp = ['time(sec)', 'abstmp(K)', 'temp(C)', 'mass-c', 'mass-h', 'mass-l']
header_dmdt = ['time(sec)', 'abstmp(K)', 'temp(C)', 'dmdt-t', 'dmdt-c', 'dmdt-h', 'dmdt-l']
```

```
header_dadt = ['time(sec)', 'abstmp(K)', 'temp(C)', 'dadt']
output_total = [0.0]*5
output_comp = [0.0]*6
output_dmdt = [0.0]*7
output_dadt = [0.0]*4
#
writer_total.writerow(header_total)
writer_comp.writerow(header_comp)
writer_dmdt.writerow(header_dmdt)
writer_dadt.writerow(header_dadt)
#
while not lstop:
   time = time + dt
   if not ltemp:
      temp = temp + dt * heat_rate / 60.
      abstemp = temp + 273.15
      if temp > end_temp:
         ltemp = True
         time_start_const = time
   else:
      temp = end_temp
      abstemp = temp + 273.15
      time_temp = time - time_start_const
      if time_temp >= time_const:
         lstop = True
#
   res_total_o = res_total
#
   res_total_cel_o = res_total_cel
   res_total_hem_o = res_total_hem
   res_total_lig_o = res_total_lig
#
   mass_cel_o = mass_cel
   mass_acel_o = mass_acel
   mass_ctar_o = mass_ctar
   mass_cchr_o = mass_cchr
   mass_cvol_o = mass_cvol
#
   mass_hem_o = mass_hem
   mass_ahem_o = mass_ahem
   mass_htar_o = mass_htar
   mass_hchr_o = mass_hchr
   mass_hvol_o = mass_hvol
#
```

```
   mass_lig_o = mass_lig
   mass_alig_o = mass_alig
   mass_ltar_o = mass_ltar
   mass_lchr_o = mass_lchr
   mass_lvol_o = mass_lvol
#
# 0:Cel -> A-Cel 1:A-Cel -> Tar 2:A-Cel -> Char+Volatiles
# 3:Hem -> A-Hem 4:A-Hem -> Tar 5:A-Hem -> Char+Volatiles
# 6:Lig -> A-Lig 7:A-Lig -> Tar 8:A-Lig -> Char+Volatiles
#
   reac_rate[0] = rung(0, time, mass_cel)
   reac_rate[1] = rung(1, time, mass_acel)
   reac_rate[2] = rung(2, time, mass_acel)
#
   reac_rate[3] = rung(3, time, mass_hem)
   reac_rate[4] = rung(4, time, mass_ahem)
   reac_rate[5] = rung(5, time, mass_ahem)
#
   reac_rate[6] = rung(6, time, mass_lig)
   reac_rate[7] = rung(7, time, mass_alig)
   reac_rate[8] = rung(8, time, mass_alig)
#
#  Calculation for mass of Cellulose
#
   mass_cel = mass_cel - reac_rate[0] * dt
   mass_acel = mass_acel \
    + (reac_rate[0] - reac_rate[1] - reac_rate[2]) * dt
   mass_ctar = mass_ctar + reac_rate[1] * dt
   mass_cchr = mass_cchr + reac_rate[2] * dt * cpr_c
   mass_cvol = mass_cvol + reac_rate[2] * dt * (1. - cpr_c)
#
#  Calculation for mass of Hemicellulose
#
   mass_hem = mass_hem - reac_rate[3] * dt
   mass_ahem = mass_ahem \
    + (reac_rate[3] - reac_rate[4] - reac_rate[5]) * dt
   mass_htar = mass_htar + reac_rate[4] * dt
   mass_hchr = mass_hchr + reac_rate[5] * dt * cpr_h
   mass_hvol = mass_hvol + reac_rate[5] * dt * (1. - cpr_h)
#
#  Calculation for mass of Lignin
#
   mass_lig = mass_lig - reac_rate[6] * dt
   mass_alig = mass_alig \
```

```
     + (reac_rate[6] - reac_rate[7] - reac_rate[8]) * dt
    mass_ltar = mass_ltar + reac_rate[7] * dt
    mass_lchr = mass_lchr + reac_rate[8] * dt * cpr_l
    mass_lvol = mass_lvol + reac_rate[8] * dt * (1. - cpr_l)
#
    res_total_cel = mass_cel + mass_acel + mass_cchr
    res_total_hem = mass_hem + mass_ahem + mass_hchr
    res_total_lig = mass_lig + mass_alig + mass_lchr
    res_total = res_total_cel + res_total_hem + res_total_lig
#
    a_old = a_now
#
    dmdt_total_cel = (res_total_cel_o - res_total_cel) / dt
    dmdt_total_hem = (res_total_hem_o - res_total_hem) / dt
    dmdt_total_lig = (res_total_lig_o - res_total_lig) / dt
    dmdt_total = (res_total_o - res_total) / dt
#
    a_now = (1. - res_total) / (1. - res_final)
    dadt = (a_now - a_old) / dt
#
#  Data output
#
    ioutput = ioutput + 1
    if ioutput == ioutput_int:
       output_total[0] = time
       output_total[1] = abstemp
       output_total[2] = temp
       output_total[3] = res_total
       output_total[4] = a_now
#
       output_comp[0] = time
       output_comp[1] = abstemp
       output_comp[2] = temp
       output_comp[3] = res_total_cel
       output_comp[4] = res_total_hem
       output_comp[5] = res_total_lig
#
       output_dmdt[0] = time
       output_dmdt[1] = abstemp
       output_dmdt[2] = temp
       output_dmdt[3] = dmdt_total
       output_dmdt[4] = dmdt_total_cel
       output_dmdt[5] = dmdt_total_hem
       output_dmdt[6] = dmdt_total_lig
```

```
#
      output_dadt[0] = time
      output_dadt[1] = abstemp
      output_dadt[2] = temp
      output_dadt[3] = dadt
#
      writer_total.writerow(output_total)
      writer_comp.writerow(output_comp)
      writer_dmdt.writerow(output_dmdt)
      writer_dadt.writerow(output_dadt)
#
      ioutput = 0
#
   if lstop:
      break
#
f_total.close()
f_comp.close()
f_dmdt.close()
f_dadt.close()
```